



HAL
open science

Spatial heterogeneity of interaction strength has contrasting effects on synchrony and stability in trophic metacommunities

Pierre Quévrex, Bart Haegeman, Michel Loreau

► To cite this version:

Pierre Quévrex, Bart Haegeman, Michel Loreau. Spatial heterogeneity of interaction strength has contrasting effects on synchrony and stability in trophic metacommunities. 2022. hal-03829838v1

HAL Id: hal-03829838

<https://hal.science/hal-03829838v1>

Preprint submitted on 25 Oct 2022 (v1), last revised 27 Jan 2023 (v3)

HAL is a multi-disciplinary open access archive for the deposit and dissemination of scientific research documents, whether they are published or not. The documents may come from teaching and research institutions in France or abroad, or from public or private research centers.

L'archive ouverte pluridisciplinaire **HAL**, est destinée au dépôt et à la diffusion de documents scientifiques de niveau recherche, publiés ou non, émanant des établissements d'enseignement et de recherche français ou étrangers, des laboratoires publics ou privés.

Spatial heterogeneity of interaction strength has contrasting effects on synchrony and stability in trophic metacommunities

Pierre Quévreux¹, Bart Haegeman¹, and Michel Loreau¹

¹*Theoretical and Experimental Ecology Station, UAR 2029, CNRS, 09200 Moulis, France*

Abstract

Spatial heterogeneity is a fundamental feature of ecosystems, and ecologists have identified it as a factor promoting the stability of population dynamics. In particular, the asymmetry of interaction strength and resource supply between patches generates an asymmetry of biomass turnover with a fast and a slow patch. The coupling of these two energy channels by mobile predators has been identified to increase stability at different scales by promoting the asynchrony of population dynamics between each patch. Here, we demonstrate that asymmetry has a contrasting effect on the stability of asymmetric metacommunities receiving localised perturbations. We built a model of an asymmetric metacommunity with two patches linked by the dispersal of predators and in which prey receive stochastic perturbations only in one patch. Perturbing prey in the fast patch synchronises the dynamics of prey biomass between the two patches and destabilises predator dynamics by increasing their temporal variability. Conversely, perturbing prey in the slow patch desynchronises their dynamics and stabilises predator dynamics. This discrepancy between the responses is due to asymmetric transmission of perturbations caused by the asymmetric distribution of biomass between the fast and the slow patch. Consequently, the fast patch drives the dynamics of the metacommunity and imposes synchrony while the slow patch does not. Therefore, local perturbations can have opposite consequences at the regional scale depending on the characteristics of the perturbed patch. Our results have strong implications for conservation ecology and suggest reinforcing protection policies in fast patches to dampen the effects of perturbations and promote the stability of population dynamics at the regional scale.

Key words

source-sink, stochastic perturbations, food chain, dispersal, asymmetry, conservation

28 Introduction

29 Since May (1972) demonstrated that stability was not an inherent property of ecological interac-
30 tion networks, ecologists have been relentlessly looking for the mechanisms ensuring ecosystem stability.
31 Spatial heterogeneity has long been identified as one of the main factors promoting the mechanisms
32 underlying the maintenance of biodiversity and the stability of ecosystems. For instance, spatial hetero-
33 geneity provides local favourable conditions to each species of the regional pool (Holt, 1984; Chesson,
34 2000; Amarasekare and Nisbet, 2001), which in turn ensures species persistence in less favourable patches
35 by source-sink dynamics (Mouquet and Loreau, 2002, 2003; Loreau et al., 2003). The stability of the
36 temporal dynamics of species biomass is ensured by the asynchrony of the dynamics between patches,
37 which leads to compensatory dynamics (Loreau et al., 2003; Loreau and de Mazancourt, 2008). There-
38 fore, spatial heterogeneity has been accepted as an element of the common wisdom on stability but the
39 models cited above relied on neutral or competitive communities and did not account for the feedbacks
40 induced by trophic interactions.

41 Inspired by the description of fast and slow energy channels by soil ecologists (*i.e.*, in terms of biomass
42 turnover), Rooney et al. (2006) noted the stabilising effect of the asymmetry of energy flows in ecosystems
43 with a food web model consisting of one mobile predator feeding on two energy channels. In their model,
44 the asymmetry of energy flow is generated by the asymmetry of interaction strength between predators
45 and prey and the asymmetry of the consumption of a common resource by the two basal species, which in
46 turn promotes the asynchrony of prey biomass dynamics in response to perturbations. However, Rooney
47 et al. (2006) and subsequent studies (Goldwyn and Hastings, 2009; Ruokolainen et al., 2011) did not iden-
48 tify the mechanisms underlying this asynchrony and the dynamics of asymmetric food webs in general.
49 Recent theoretical studies were able to accurately explain the synchrony patterns in metacommunities
50 (Quévreux et al., 2021a,b), and we propose to consider the effects of asymmetry from the metacommunity
51 perspective to fill this gap.

52

53 Metacommunities embody the spatial dimension of interaction networks: they consist of distant patches
54 connected by the dispersal of the organisms living in each patch (Leibold et al., 2004; Leibold and Chase,

corresponding author: pierre.quevreux@cri-paris.org

55 2017). The metacommunity framework is particularly suitable to represent the spatial heterogeneity
56 observed in ecosystems because each community has its own characteristics such as biomass turnover.
57 Following Rooney et al.'s (2006) model, many studies varied the asymmetry of interaction strength and/or
58 resource supply to manipulate the difference in biomass turnover between the energy channels hosted by
59 each patch (Goldwyn and Hastings, 2009; Ruokolainen et al., 2011; Anderson and Fahimipour, 2021).
60 More generally, interaction strength is key in community dynamics because it governs food web structure,
61 stability (Neutel et al., 2002) and biomass distribution (Barbier and Loreau, 2019) by simultaneously de-
62 termining predator growth and prey mortality. Therefore, its significant variations observed in nature,
63 often reported as predation risk by prey in field studies (Table 1), should lead to dramatic variations in
64 community functioning across space.

65

66 In addition to the asymmetry of interaction strength, Rooney et al. (2006) highlighted the importance
67 of mobile predators coupling two different energy channels, a keystone role in ecosystem functioning
68 largely reported by empirical studies (Schindler and Scheuerell, 2002; Vadeboncoeur et al., 2005; Olf
69 et al., 2009; Dolson et al., 2009). Rooney et al. (2006) explained the increase in food web stability with
70 asymmetry by the asynchronous response of prey to the perturbation of the predator. Indeed, small
71 spatial heterogeneity can lead to strong asynchrony in oscillating predator-prey systems (Goldwyn and
72 Hastings, 2009), but Ruokolainen et al. (2011) identified a humped-shaped relationship in which only
73 moderate asymmetry generates a maximum of stability (a lower coefficient of variation of biomass in
74 their study), which suggests that the effects of asymmetry on stability are not trivial. Several major gaps
75 limit our understanding of the consequences of asymmetry on metacommunity stability. First, the mech-
76 anisms linked to asymmetry and promoting asynchrony are not identified. Second, the way perturbations
77 propagate in heterogenous metacommunities remains unknown. Stability patterns are tightly linked to
78 synchrony patterns since the asynchrony of local population dynamics leads to more stable dynamics (low
79 biomass CV) at higher scales due to compensatory dynamics (Loreau et al., 2003; Gonzalez and Loreau,
80 2008; Loreau and de Mazancourt, 2013; Wilcox et al., 2017). However, Quévreux et al. (2021a) showed
81 that the perturbation and dispersal of particular trophic levels govern synchrony and stability in sym-
82 metric metacommunities. Therefore, we expect asymmetric effects of perturbations affecting particular
83 patches.

84

85 Here, we expect that asymmetry is not a generic stabilising factor, as claimed by previous works

Table 1: Approximative relative increase in predation risk between low-risk and high-risk environments (equivalent to the asymmetry of interaction strength γ in Figure 1). See Gorini et al. (2012) for an extended review and more references.

Predator	Prey	γ	Reference
American marten	Vole species	1.6	Andruskiw et al., 2008
Wolf	Moose	14-100	Gervasi et al., 2013
Wolf	Roe deer	2.5-8	Gervasi et al., 2013
Wolf	Elk	10	Kauffman et al., 2007
Savannah predators	Savannah ungulates	1.5-4.5	Thaker et al., 2011
Artificial gecko	Australian predators	2.8	Hansen et al., 2019
Lynx	Roe deer	2	Gehr et al., 2020
Puma	Vicuña	1.6	Donadio and Buskirk, 2016

86 (Rooney et al., 2006; Goldwyn and Hastings, 2009; Ruokolainen et al., 2011), but strongly depends on
87 which patch is perturbed according to its characteristics. To explore this statement, we consider a simple
88 metacommunity model of two patches hosting a predator-prey couple and with asymmetric interaction
89 strength and resource supply. The stability of the metacommunity is assessed by the response at different
90 scales when prey receive stochastic perturbations in one of the two patches. We show contrasting effects
91 of asymmetry: perturbing prey in the fast patch (equivalent to the fast channel defined by Rooney and
92 McCann, 2012) promotes prey synchrony and decreases predator stability at the metapopulation scale
93 while perturbing the slow patch has the opposite effects.

94 Methods

95 Metacommunity model

We use the model proposed by Quévieux et al. (2021a) based on the food chain model developed by Barbier and Loreau (2019). The model consists of two patches that each sustain a food chain with Lotka-Volterra predator-prey interactions (equations (1a) and (1b)).

$$\frac{1}{D} \frac{dB_1^{(1)}}{dt} = B_1^{(1)} \left(\omega \frac{g}{D} - B_1^{(1)} - \gamma ma B_2^{(1)} \right) \quad (1a)$$

$$\frac{1}{mD} \frac{dB_2^{(1)}}{dt} = \underbrace{B_2^{(1)} \left(-B_2^{(1)} + \gamma \epsilon a B_1^{(1)} \right)}_{\text{intra-patch dynamics}} + \underbrace{d_2 \left(B_2^{(2)} - B_2^{(1)} \right)}_{\text{dispersal}} \quad (1b)$$

96 Prey have a positive effect ϵa on predators (ϵ is the conversion efficiency and a is the interspecific
97 interaction rate relative to intraspecific interactions), and predators have a negative effect ma on prey (m
98 is the predator to prey metabolic rate ratio)(Figure 1A). The time scale of the system is rescaled by the

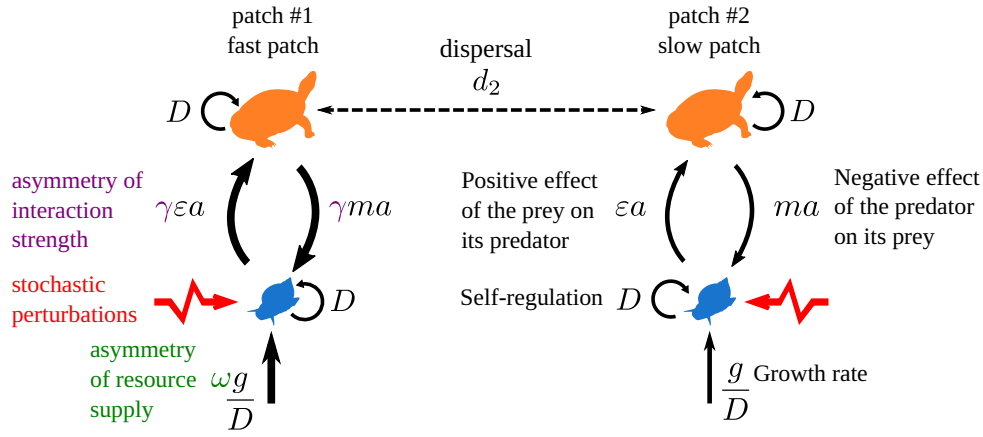


Figure 1: The metacommunity model consists of two patches, each sustaining a predator-prey couple linked by predators, which disperse at a very high scaled rate d_2 . Prey grow at a rate g/D and have a positive effect εa on predators, while predators have a negative effect ma on prey. Each species population is also limited by self-regulation D (negative intraspecific interactions). Spatial heterogeneity is embodied by the asymmetry of resource supply (green) and the interaction strength (purple), which are higher in patch #1 by factors ω and γ , respectively. Consistent with Rooney et al. (2006), patch #1 is called the fast patch, and patch #2 is called the slow patch. Prey receive stochastic perturbations either in patch #1 or in patch #2 (red arrows).

99 metabolic rate of prey, and biologic rates of each species i are rescaled by its intraspecific interaction rate
 100 D_i . Therefore, we obtain the relative growth rate g/D and the scaled dispersal rate d_i (see Appendix S1-1
 101 for a detailed description of the rescaling). Considering scaled parameters and aggregated parameters
 102 (εa and ma) enables us to explore a wide range of ecological situations. We do not describe the food
 103 web model in detail because it is not required to understand our results but a thorough description is
 104 available in Appendix S1-1. Parameters and their values are summarised in Table 2.

105 Predators disperse at a very high scaled rate d_2 and strongly couple the two patches. As in Rooney et
 106 al. (2006), resource supply and interaction strength are asymmetric between patches since they are higher
 107 in patch #1 by factors γ and ω respectively (Figure 1B). Patch #1 corresponds to the fast energy channel,
 108 in which biomass has a high turnover, while patch #2 corresponds to the slow channel. Therefore, we
 109 call patch #1 the fast patch and patch #2 the slow patch. We set $\gamma = \omega$ to ensure species persistence
 110 over the entire range of parameters (see Figure S2-3 in the supporting information) but varying them
 111 independently does not qualitatively change the results (see Figure S2-11 in the supporting information).
 112 In the following, we only refer to γ for the sake of simplicity and only consider $\gamma \geq 1$ because $\gamma \leq 1$ just
 113 swaps the roles of patches #1 and #2.

114 Response to stochastic perturbations

115 We use the same methods as Quévieux et al. (2021a) to study the response of metacommunities to
 116 stochastic perturbations. Indeed, recent studies advocate for the use of the temporal variability of biomass

117 (Haegeman et al., 2016; Arnoldi et al., 2018), which is measured by the coefficient of variation (CV), and
 118 can be easily measured experimentally. In addition, Wang and Loreau (2014, 2016), Wang et al. (2019),
 119 and Jarillo et al. (2022) showed that CVs scale up from local populations to community, regional and
 120 metacommunity levels, therefore providing a comparison of stability at different scales. Here, we provide
 121 only a brief description of the main concepts, but a thorough description is available in Appendix S1.

Prey in the fast or slow channel receive stochastic perturbations that are represented by equation (2).

$$dB_i = \underbrace{f_i(B_1, \dots, B_S)dt}_{\text{Deterministic}} + \underbrace{\sigma_i \sqrt{B_i^*} dW_i}_{\text{Perturbation}} \quad (2)$$

122 $f_i(B_1, \dots, B_S)$ represents the deterministic part of the dynamics of species i , as described by equations (1a)
 123 and (1b)). Stochastic perturbations are defined by their standard deviation σ_i and dW_i , a white noise
 124 term with a mean of 0 and variance of 1. Perturbations also scale with the square root of the biomass at
 125 equilibrium B_i^* of the perturbed population. Such scaling makes the perturbations similar to demographic
 126 stochasticity (from birth-death processes) that evenly affect each species regardless of abundance (Arnoldi
 127 et al., 2019). In other words, the ratio of species biomass variance to perturbation variance is roughly
 128 independent of biomass, which disentangles the effect of asymmetry on perturbation transmission from
 129 its effect on species abundance.

In the following, we assess the temporal variability of each population after stochastic perturbations
 affect the metacommunity in the vicinity of equilibrium. Therefore, we linearise the system in the vicinity
 of equilibrium to obtain equation (3) where $X_i = B_i - B_i^*$ is the deviation from equilibrium.

$$\frac{d\vec{X}}{dt} = J\vec{X} + T\vec{E} \quad (3)$$

130 J is the Jacobian matrix, which represents the linearised direct effects between populations in the vicinity
 131 of equilibrium, and T defines how the perturbations $E_i = \sigma_i dW_i$ apply to the system (*i.e.*, which species
 132 they affect and how they scale with biomass, where T is a diagonal matrix whose terms are $T_{ii} = \sqrt{B_i^*}$).

We then obtain the variance-covariance matrix C^* of species biomasses (variance-covariance matrix of
 \vec{X}) from the variance-covariance matrix of perturbations V_E (variance-covariance matrix of \vec{E}) by solving
 the Lyapunov equation equation (4) (Arnold, 1974; Wang et al., 2015; Arnoldi et al., 2016; Quévieux

Table 2: Table of parameters. σ_i is set very small to keep the system in the vicinity of equilibrium. More combinations of εa and ma are tested in the supporting information. d_2 is set very high to emphasise the high mobility of predators and their ability to couple prey populations. ω is set equal to γ .

parameter	interpretation	value
σ_i	standard deviation of stochastic noise	10^{-3}
g	net growth rate of prey	1
r	death rate of predators	0
D	self-regulation	1
ϵ	conversion efficiency	0.65
m	predator/prey metabolic rate ratio	0.65
a	attack rate	1.54,
εa	positive effect of prey on predators	1
ma	negative effect of predators on prey	1
d_2	scaled dispersal rate of predators	10^6
ω	asymmetry of resource supply	[1,10]
γ	asymmetry of interaction strength	[1,10]

et al., 2021a).

$$JC^* + C^*J^\top + TV_E T^\top = 0 \quad (4)$$

133 The expressions for V_E and T and the method to solve the Lyapunov equation are detailed in Appendix S1-
134 5. From the variance-covariance matrix C^* , we compute the coefficient of correlation of the biomass
135 dynamics between the two populations of each species (see equation (20) in the supporting information)
136 and we measure the stability with the coefficient of variation (CV) of the biomass. In addition, biomass
137 CVs can be measured at different scales: population scale (*e.g.*, biomass CV of prey in patch #1),
138 metapopulation scale (*e.g.*, CV of the total biomass of prey) and metacommunity scale (*e.g.*, CV of
139 the total biomass of predator and prey put together) to assess the effects of asymmetry at local and
140 regional scales (Figure 4A and see Appendix S1-6). Finally, we quantify the synchrony of the dynamics
141 of the different populations with the coefficient of correlation, which is also computed from the variance-
142 covariance matrix C^* (Appendix S1-6).

143 Results

144 Source-sink effect

145 In the following, we consider a metacommunity in which only predators are able to disperse ($d_2 = 10^6$)
146 to be consistent with the common observations of predators coupling different energy channels, which can
147 differ in their energy turnover with a fast patch (patch #1 here) and a slow patch (patch #2, see Figure 1).

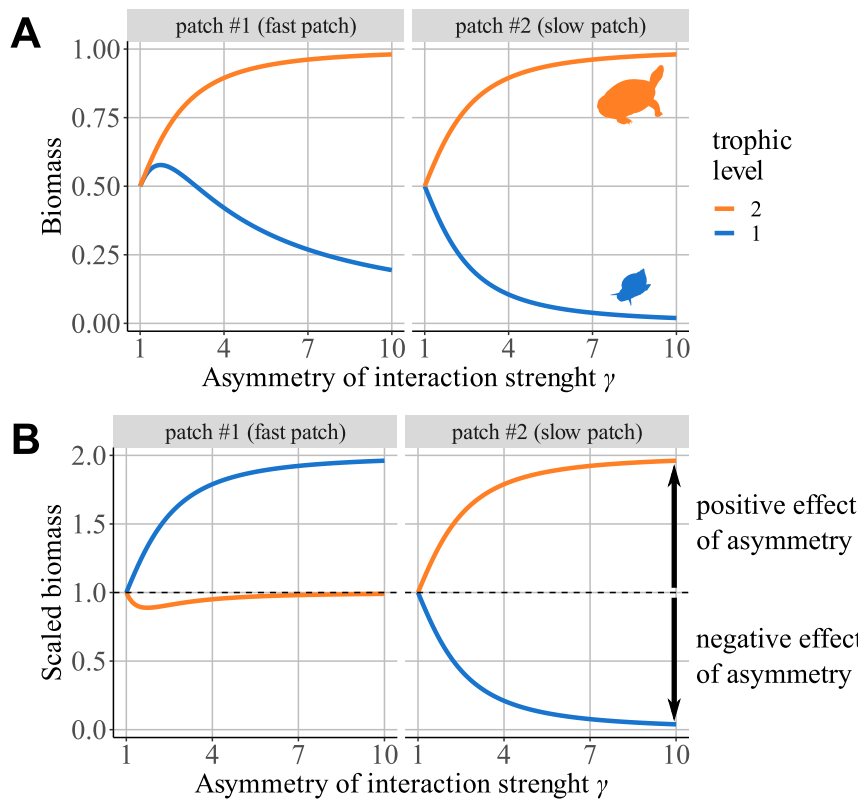


Figure 2: **A**) Distribution of the biomass of each species among patches depending on the asymmetry of interaction strength γ . **B**) Distribution of biomasses scaled by their value in a metacommunity without dispersal ($B_{scaled} = B_{d_2>0}/B_{d_2=0}$).

148 Varying the asymmetry of interaction strength γ is equivalent to varying the interaction strength a in
 149 patch #1 and has the same effects on species biomass: first increasing γ increases predator biomass by
 150 increasing prey consumption, then it decreases predator biomass because of resource overexploitation
 151 (Figure S2-2 in the supporting information). This leads to different biomass distributions in patches #1
 152 and #2 (Figure 2A). Predator biomass increases with γ and is the same in both patches because their
 153 high dispersal rate balances any difference. Prey biomass is higher in patch #1 than in patch #2, and
 154 both decrease with γ , except in patch #1, where we first observe a small increase for $\gamma < 2$. This response
 155 is due to source-sink effects: the increase in prey consumption in patch #1 increases predator biomass
 156 (source) that spills over patch #2 (sink) due to dispersal (Figure 2B and Figure 6A). Therefore, predator
 157 biomass is lower in patch #1 and higher in patch #2 compared to what we expect in the same food chains
 158 in isolation (*i.e.*, without dispersal). This also prevents predators from overexploiting prey in patch #1
 159 by spreading the increased predator biomass across the metacommunity, which explains why we do not
 160 observe a decrease in predator biomass for high values of γ , as shown in Figure S2-2. Conversely, the
 161 distribution of prey biomass across the two patches is opposite (higher in patch #1 and lower in patch
 162 #2).

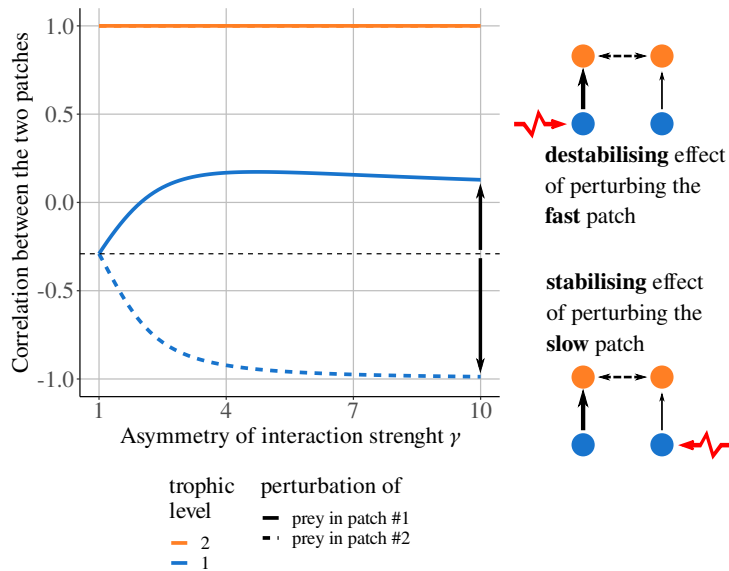


Figure 3: Spatial correlation between the populations of each species depending on asymmetry of interaction strength γ when predators disperse and prey are perturbed in patch #1 or #2. The dashed line emphasises the value of the correlation of prey populations without asymmetry ($\gamma = 1$).

Effects on stability

Now, we describe how asymmetry of interaction strength γ shapes metacommunity stability at different scales. Since predators have a very high scaled dispersal rate ($d_2 = 10^6$), their populations are perfectly correlated and display the same dynamics. Our main result is that prey become more correlated when they are perturbed in patch #1 (fast channel in which $\gamma > 1$), while they become more anticorrelated when they are perturbed in patch #2 (Figure 3). Increasing γ amplifies the difference in correlation between these two scenarios, and this pattern qualitatively holds for various combinations of the physiological and ecological parameters εa and ma (see Figure S2-6 in the supporting information).

Increasing the asymmetry of interaction strength γ has contrasting effects on biomass CV as well. At the population scale, it increases the biomass CV of each population when prey are perturbed in the fast patch (Figure 4B). When prey are perturbed in the slow patch, increasing γ slightly alters the biomass CV of prey in patch #1, increases the biomass CV of prey in patch #2 and decreases the biomass CV of predators. This discrepancy can be attributed to the strong effect of γ on prey biomass in patch #2 (Figure 2A): prey biomass strongly decreases with γ in patch #2, which increases their biomass CV.

At the metapopulation scale, the asymmetry of interaction strength γ increases the biomass CV of prey in both scenarios of perturbation (Figure 4C). However, this result is not true for all values of εa and ma (Figure S2-7A in the supporting information) because of the various responses of prey biomass to γ among patches (Figure S2-5A in the supporting information). The biomass CV of predators is higher

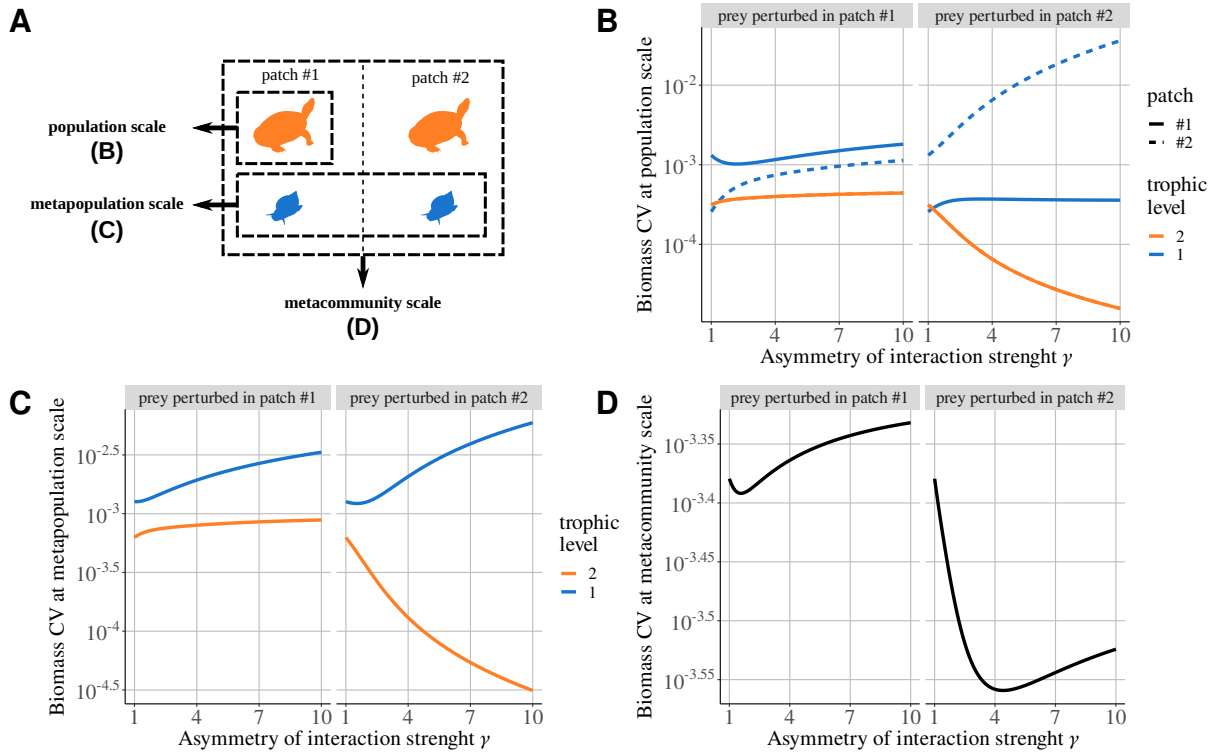


Figure 4: Stability at different scales depending on asymmetry of interaction strength γ when predators disperse and prey are perturbed in patch #1 or #2. **A)** The temporal variability in the metacommunity is assessed by the coefficient of variation (CV) of biomass at different scales: population scale (biomass CV of one species in one patch), metapopulation scale (CV of the total biomass of one species across patches) and metacommunity scale (CV of the total biomass of the entire metacommunity). **B)** Biomass CV at the population scale. **C)** Biomass CV at the metapopulation scale (CV of the total biomass of each species). **D)** Biomass CV at the metacommunity scale (CV of the total biomass of the metacommunity).

181 when prey are perturbed in the fast patch (patch #1) compared to the case in which prey are perturbed
 182 in the slow patch (#2) (Figure 4C), which is consistent for all values of εa and ma (see Figure S2-7A in
 183 the supporting information).

184 Finally, stability at the metacommunity scale depends on the distribution of biomass and CV among
 185 species. In our case ($\varepsilon a = 1$ and $ma = 1$), predators have the largest total biomass (Figure 2A) and
 186 drive the biomass CV at the metacommunity scale for low values of asymmetry of interaction strength
 187 γ (Figure 4D). For high values of γ , when prey are perturbed in patch #2, the CV of total biomass
 188 increases with γ because it is driven by prey in patch #2, whose biomass CV is much higher than the
 189 biomass CV of predators, which compensates for their lower biomass.

190 Underlying mechanisms

191 To unveil the mechanisms governing the stability of heterogeneous metacommunities, we look deeper
 192 into the dynamics after a pulse perturbation (Figure 5A) and explain them with the direct effects between
 193 species quantified by the Jacobian matrix (see equation (3)). When the perturbation of prey occurs in

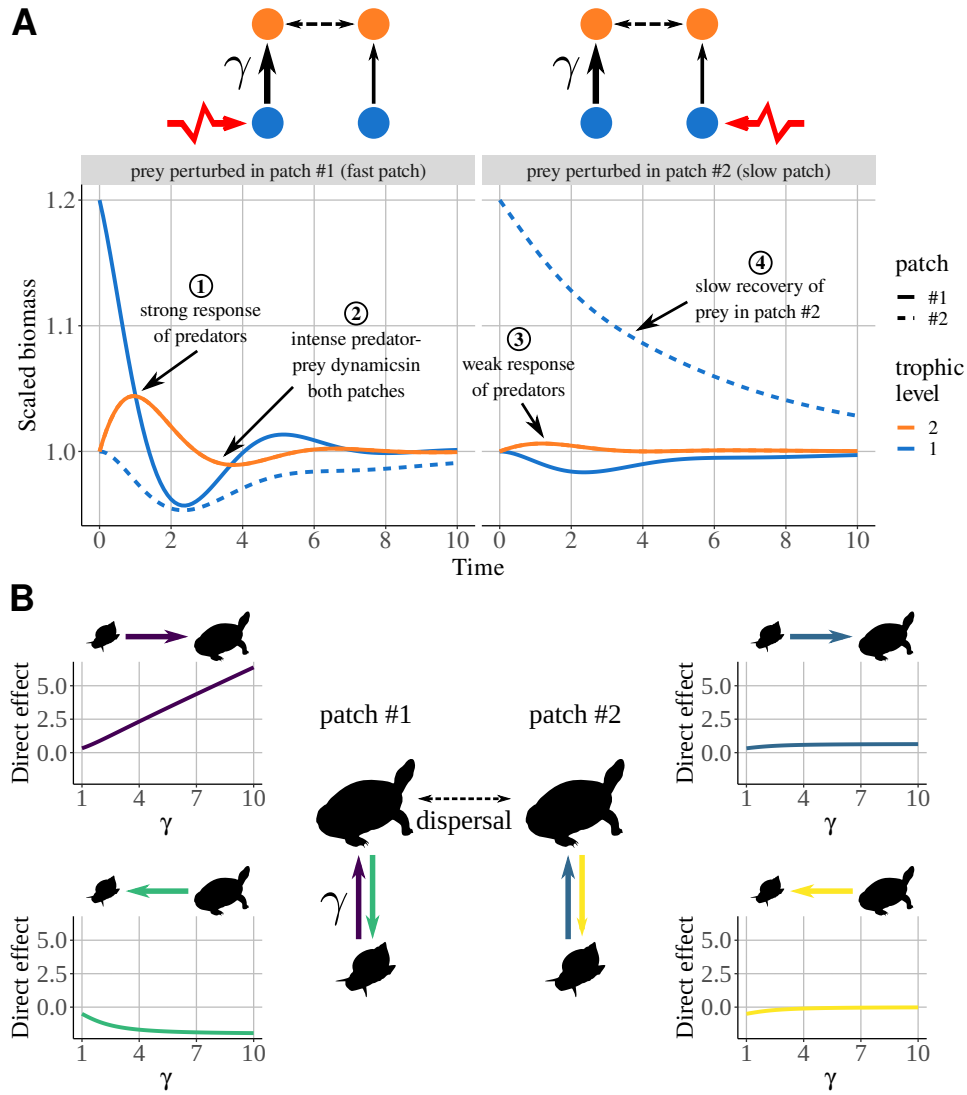


Figure 5: **A**) Time series of biomasses rescaled by their value at equilibrium after an increase of 20% in prey biomass in patch #1 (left panel) or patch #2 (right panel) for a value of interaction strength asymmetry $\gamma = 3$. **B**) Direct effect of prey on predator (and vice versa) depending on interaction strength asymmetry γ . Direct effects correspond to the terms of the Jacobian matrix.

194 patch #1, the strong direct effect of prey on predators (and vice versa) in patch #1 due to γ (Figure 5B)
 195 leads to a strong response of predators ①, which in turn drives the response of the two prey popu-
 196 lations ②. In detail, predator biomass in patch #1 first increases because of the abundance of prey.
 197 Then, predators deplete prey biomass in both patches and correlate their dynamics, which explains why
 198 asymmetry of interaction strength γ increases prey correlation when prey are perturbed in patch #1.

199 When the perturbation of prey occurs in patch #2, the weak direct effect of prey on predators (Fig-
 200 ure 5B) leads to a small response of predators ③. In turn, the very low direct effect of predators on
 201 prey in patch #2 does not allow perturbations to ripple back to patch #2 where prey slowly recover from
 202 the initial perturbation ④ (Figure 6B). This slow recovery is emphasised by the source-sink dynamics
 203 in the metacommunity (Figure 6A), which leads to a lower biomass of prey in patch #2 compared to

204 a metacommunity without dispersal, therefore decreasing biomass flows in patch #2 and its recovery
205 speed. This difference in recovery speed between patches #1 and #2 leads to the anti-correlation of prey
206 populations because it increases the time interval in which they have opposite variations: an increase in
207 the biomass of prey in patch #1, which follows the initial decrease due to predation, and a slow decrease
208 in prey biomass in patch #2.

209 In summary, the asymmetry of interaction strength alters the biomass distribution among trophic
210 levels in each patch (Figure 6A), which leads to strong predator-prey interactions in the fast patch and
211 weak interactions in the slow patch (Figure 6B). Therefore, if the fast patch is perturbed, it drives the
212 dynamics of the slow patch and synchronises prey dynamics. Conversely, the perturbation of the slow
213 patch does not significantly affect the fast patch, and both independently recover from perturbations,
214 which desynchronises prey dynamics.

215 Discussion

216 We have shown that the asymmetry of interaction strength has contrasting effects on stability de-
217 pending on which patch is perturbed. Perturbing prey in the fast patch (in which interaction strength is
218 the highest) tends to synchronise the dynamics of prey biomass and increases the temporal variability of
219 predator dynamics at the metapopulation scale, while perturbing prey in the slow patch desynchronises
220 prey dynamics and decreases the temporal predator dynamics. This discrepancy between the responses
221 is due to asymmetric transmission of perturbations within each patch, itself caused by the alteration of
222 biomass distribution and the asymmetry of interaction strength (Figure 6A). Perturbations are strongly
223 transmitted from the fast patch to the slow patch, while the reverse transmission is weak (Figure 6B).
224 Consequently, the fast patch drives the dynamics of the metacommunity and synchronises prey dynam-
225 ics, while the slow patch does not, and the almost independent recovery from perturbation in each patch
226 desynchronises prey dynamics.

227 Stability in a heterogeneous world

228 Our results show that spatial heterogeneity, which is represented by the asymmetry of interaction
229 strength and resource supply as in Rooney et al. (2006), generates mechanisms that alter local and re-
230 gional dynamics, which deeply changes the synchrony of population dynamics and the stability of the
231 metacommunity at different scales. In a homogeneous metacommunity, the spatial correlation of the

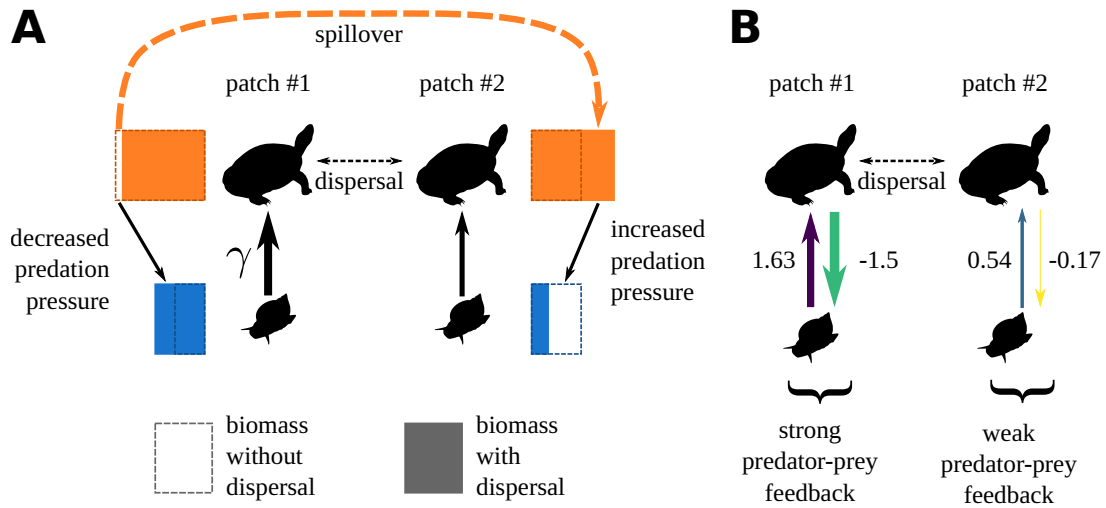


Figure 6: Mechanisms leading to the spatial synchrony of prey dynamics when prey are perturbed in the patch with the strongest interaction strength (patch #1 with $\gamma = 3$). **A**) Asymmetry in interaction strength alters the biomass distribution between the two patches. Increased interaction strength in patches #1 enhances the biomass production of predators that spill over patches from patch #1 to patch #2, therefore increasing prey biomass in patch #1 and decreasing it in patch #2. Plain rectangles represent the biomass of each population, while dashed rectangles represent the same population in a metacommunity without dispersal (no spillover effect). **B**) The asymmetry of biomass distribution and interaction strength alters the direct effects between predators and prey. High prey density and high interaction strength promote strong feedback in patch #1, which promotes the transmission of perturbations when prey are perturbed in patch #1. Low prey density and low interaction strength promote a weak feedback in patch #2, which limits the transmission of perturbations when prey are perturbed in patch #2. The discrepancy between the feedback strengths explains the synchrony of prey dynamics: when prey are perturbed in patch #1, the predator-prey couple in patch #1 has an overwhelming impact on the metacommunity and drives the dynamics in patch #1, which leads to synchrony of prey populations. Conversely, perturbing prey in patch #2 has a minor impact on dynamics in patch #1, which decreases the synchrony of prey populations.

232 dynamics of the different populations of each species can be assessed from the correlation of the different
 233 species within each patch, the dispersing species making the link between the correlation patterns (see
 234 Figure S2-25 for a summary of the results of Quévieux et al., 2021a). In other words, knowledge of
 235 the dynamics at the local scale is enough to completely understand the stability pattern at the meta-
 236 community scale. In a heterogeneous metacommunity, such a simple framework does not hold because
 237 each patch does not contribute equally to the dynamics due to the overwhelming influence of the fast
 238 patch (see Figure S2-4 in the supporting information). Rooney et al. (2006) verbally explained that each
 239 patch has dynamics with different speeds: the fast channel (with higher interaction rates and resource
 240 supplies) enables a quick recovery after a perturbation while the slow channel dampens the dynamics
 241 in the long term and prevents the system from overshooting. Here, we demonstrate that stability is
 242 driven by the mechanisms responsible for the synchrony of prey populations. Perturbations are strongly
 243 transmitted from prey to predator in the fast patch, which enables strong transmission to the slow patch
 244 and therefore synchronises the dynamics of prey populations (Figure 6B). Conversely, perturbations are
 245 poorly transmitted within the slow patch, which leads to the asynchrony of prey populations due to the

246 independent recovery in each patch. Undoubtedly, the dynamics at the metacommunity scale cannot be
247 assessed by the dynamics at the local scale, as in Quévreur et al. (2021a), and they are an emergent
248 property resulting from the tight interplay between the strength of perturbation transmission in each
249 patch.

250 Our description of the mechanisms underlying the apparent stabilising effects of spatial heterogeneity
251 should enlighten the results of previous theoretical studies. Goldwyn and Hastings (2009) and Ruoko-
252 lainen et al. (2011) found that the asymmetry of interaction rate leads to asynchrony by generating
253 out-of-phase dynamics in a system with endogenous oscillations. In particular, Ruokolainen et al. (2011)
254 found a U-shaped relationship: for moderate asymmetry, the spatial asynchrony of predator and prey
255 populations is maximal, which leads to optimum stability at the metacommunity scale. Our results
256 suggest that moderate asymmetry would alter the phase of the oscillations in each patch while keeping
257 the amplitude of oscillations equivalent, therefore promoting asynchrony. Conversely, a strong asym-
258 metry would increase the imbalance between oscillation amplitude and enable the fast patch to take
259 over the slow patch, which would bring back synchrony. However, their results rely on phase-locking
260 (Jansen, 1999; Lloyd and May, 1999; Goldwyn and Hastings, 2008; Vasseur and Fox, 2009), which is
261 the coupling of the phase of oscillators embodied by predator-prey pairs in each patch. Although our
262 results provide interesting insight into metacommunity dynamics, they cannot grasp the fine mechanisms
263 underlying nonlinear phenomena such as phase-locking and further studies are needed to identify these
264 mechanisms. Finally, most of the theoretical studies consider the effect of spatial heterogeneity combined
265 with variations in dispersal rate (Gravel et al., 2016; Anderson and Fahimipour, 2021) or habitat choice
266 by predators (Rooney et al., 2006; Ruokolainen et al., 2011), therefore confounding the fundamental
267 effects of asymmetry. We have identified the mechanisms linked to asymmetry, but future work must
268 now investigate their interactions with other processes such as density-dependent dispersal.

269 **Generality of the effects of asymmetry on stability**

270 Our main results is that asymmetry is stabilising when the slow patch is perturbed, while it is desta-
271 bilising when the fast patch is perturbed. This result is strikingly robust to several deviations from the
272 original model we have described. First, we show that the described mechanisms are valid for a wide range
273 of ecological and physiological parameters leading to various distributions of biomass among predators
274 and prey (see Figures S2-5 and S2-6 in the supporting information). In addition, we observe the same
275 results for longer food chains as long as prey populations are directly coupled by the dispersing predator

276 (see Figures S2-15 and S2-16 in the supporting information). Currently, we do not identify a clear pat-
277 tern for species lower in the food chain over a wide range of ecological and physiological parameters but
278 further studies are needed to investigate the potential indirect effects propagating across the food chain.
279 Second, the mechanisms are not restricted to prey populations coupled by a mobile predator but also
280 apply to predator populations coupled by a mobile prey (see Figure S2-19 in the supporting information).
281 Therefore, we anticipate that mobile predators are not the only major drivers of synchrony and stability
282 in ecosystems (Schindler and Scheuerell, 2002; Vadeboncoeur et al., 2005; Dolson et al., 2009; Olf et al.,
283 2009; Rooney and McCann, 2012), and resource species may also have an equivalent impact. Taken
284 together, these two points strongly suggest that the mechanisms underlying stability and synchrony in
285 response to perturbations should be general to metacommunities regardless of the ecological parameters,
286 biomass distribution and dispersal among species.

287 Spatial heterogeneity has often been presented as a generic condition generating mechanisms ensuring
288 stability, but our results contradict this statement. The models focusing on the asymmetric feeding of
289 consumers on different energy channels or different patches showed that it promotes the existence of
290 stable equilibria (McCann et al., 1998), greater asymptotic resilience (Rooney et al., 2006), asynchrony
291 of prey in response to predator perturbation (Rooney et al., 2006) and out-of-phase limit cycles (Gold-
292 wyn and Hastings, 2009; Ruokolainen et al., 2011). McCann et al. (1998) and Ruokolainen et al. (2011)
293 only observed the stabilising effect for moderate spatial heterogeneity, but it remains a stabilising factor
294 nonetheless. All these studies considered measures of stability aiming to capture the general stability
295 properties of metacommunities and miss the targeted effects of perturbations. Rooney et al. (2006) only
296 considered the perturbation of the mobile predator and ignored the specific perturbation of the fast or
297 slow channels. Although asymmetry does not necessarily promote stability, our results show that gen-
298 eral mechanisms drive the response of metacommunities to localised perturbations, therefore providing a
299 valuable framework to assess the response of ecosystems to localised perturbations due to human activity.
300 Additionally, these mechanisms enable us to understand the effect of environmental perturbations affect-
301 ing all patches. As demonstrated by Arnoldi et al. (2019), environmental perturbations affect abundant
302 populations the most, which is the prey population in the fast patch in our case (see Figure S2-22 in
303 the supporting information). Therefore, we anticipate that the fast patch will govern the dynamics of
304 metacommunities in which all populations are perturbed (see Figure S2-24 in the supporting information).

305 Implications for conservation

306 The metacommunity framework has long been used in conservation ecology (Johnson et al., 2013;
307 Patrick et al., 2021). Conservation efforts are usually concentrated on particular locations and useful
308 management must consider the ecological processes acting at the landscape scale (Van Teeffelen et al.,
309 2012; Chase et al., 2020). For instance, spatial heterogeneity is key to ensuring species coexistence and
310 diversity at the regional scale, which ultimately provides important ecosystem services in agricultural
311 landscapes (Bennett et al., 2006). A large corpus of theoretical studies explored the local recovery of
312 communities in a landscape receiving perturbations (Mouquet et al., 2011; Economo, 2011; Holyoak et
313 al., 2020; Jacquet et al., 2022). However, these studies focus on extinction events recovered by dispersal
314 events in a patch dynamics framework, and little is known about the effect of moderate or small pertur-
315 bations. In this context, the present study provides valuable insight into fine-scale dynamics in response
316 to perturbations.

317 Our results show that species interactions are a major driver of synchrony in heterogeneous metacom-
318 munities. Even if the species of interest does not disperse significantly, the synchrony of the dynamics
319 of its different populations can strongly depend on the interactions with another species with a higher
320 dispersal across the landscape. For instance, Howeth and Leibold (2013) showed that predatory fish
321 promote the asynchrony of oscillating populations of zooplankton in a mesocosm experiment. Therefore,
322 species endorsing this role are called "mobile link organisms" (Lundberg and Moberg, 2003) and are par-
323 ticularly targeted by conservation policy because they have major impacts on community dynamics and
324 ecosystem functioning (Soulé et al., 2005; Brodie et al., 2018). Such a species can be considered keystone
325 species (Mills and Doak, 1993) and must be clearly identified to properly manage the conservation of
326 the other interaction species. However, our results show that mobile link organisms are not the only
327 driver of metacommunity stability, and the patch being perturbed also has a major impact. The concept
328 of a keystone community, defined by Mouquet et al. (2013) for communities whose destruction causes
329 species extinction or a decrease in biomass production, can be applied to better assess the stability of
330 metacommunities. Therefore, identifying the communities living in fast and slow patches should be key
331 for conservation management aiming to mitigate the effects of perturbations.

332 According to our results, mitigating the effects of perturbations affecting the patch in which interaction
333 strength is the highest is critical to avoid the synchrony of prey dynamics (Figure 3) and ensure predator
334 stability (Figure 4C). Then, the patch in which the interaction strength between the species of interest

335 and the mobile link organism is the highest must be identified. Conservation policies usually target
336 preserved areas because they are characterised by high species richness but identifying them as fast or
337 slow patches is not trivial. Urban ecology is a relevant example because many species dwell in cities and
338 less anthropised ecosystems (*e.g.*, agricultural and natural landscapes). Urban areas can be considered
339 fast patches because of the abundance of resources (parameters ω in our model) for opportunistic species,
340 but they can also be considered slow patches because of the reduced predation pressure (parameter γ in
341 our model), cities acting as safe spaces (see Shochat et al. (2006) and Shochat et al. (2010) for review).
342 Typically, birds and rodents can find plenty of food due to human wastes, public parks and feeding while
343 experiencing less predation (Rebolo-Ifrán et al., 2017). Therefore, focusing conservation efforts on urban
344 areas to mitigate the perturbations affecting their ecosystem may be as important as protecting wild
345 areas to protect species at the metapopulation scale.

346 Conclusion

347 Asymmetry of interaction strength, and spatial heterogeneity in general, is not stabilising factor *per*
348 *se* because perturbing prey in the fast patch leads to the synchrony of the dynamics of prey populations
349 and increases the temporal variability of the mobile predator linking the two patches. Therefore, the
350 response of metacommunities to perturbations is strongly context dependent, *i.e.*, a good knowledge of
351 the characteristics of each patch relative to each other is required to assess stability at the metacommunity
352 scale. Based on our findings, we advocate for conservation efforts to target key patches not only according
353 to species richness or biomass density but also according to the distribution of interaction strength across
354 the metacommunity.

355 Acknowledgements

356 This work was supported by the TULIP Laboratory of Excellence (ANR-10-LABX-41) and by the
357 BIOSTASES Advanced Grant, funded by the European Research Council under the European Union's
358 Horizon 2020 research and innovation programme (666971).

359 Data accessibility

360 The R codes to reproduce the results and the figures are available on GitHub ([https://github.com/
361 PierreQuevreur/model_metacommunity_spatial_heterogeneity](https://github.com/PierreQuevreur/model_metacommunity_spatial_heterogeneity)).

References

- 362
- 363 Amarasekare, P., & Nisbet, R. M. (2001). Spatial heterogeneity, source-sink dynamics, and the local coexistence of competing
364 species. *The American Naturalist*, *158*(6), 572–584. <https://doi.org/10.1086/323586>
- 365 Anderson, K. E., & Fahimipour, A. K. (2021). Body size dependent dispersal influences stability in heterogeneous meta-
366 communities. *Scientific Reports*, *11*(1), 17410. <https://doi.org/10.1038/s41598-021-96629-5>
- 367 Andruskiw, M., Fryxell, J. M., Thompson, I. D., & Baker, J. A. (2008). Habitat-mediated variation in predation risk by the
368 american marten. *Ecology*, *89*(8), 2273–2280. <https://doi.org/10.1890/07-1428.1>
- 369 Arnold, L. (1974). *Stochastic differential equations: Theory and applications*. Wiley.
- 370 Arnoldi, J.-F., Bideault, A., Loreau, M., & Haegeman, B. (2018). How ecosystems recover from pulse perturbations: A
371 theory of short- to long-term responses. *Journal of Theoretical Biology*, *436*, 79–92. <https://doi.org/10.1016/j.jtbi.2017.10.003>
- 372
- 373 Arnoldi, J.-F., Loreau, M., & Haegeman, B. (2016). Resilience, reactivity and variability: A mathematical comparison of
374 ecological stability measures. *Journal of Theoretical Biology*, *389*, 47–59. <https://doi.org/10.1016/j.jtbi.2015.10.012>
- 375
- 376 Arnoldi, J.-F., Loreau, M., & Haegeman, B. (2019). The inherent multidimensionality of temporal variability: How common
377 and rare species shape stability patterns (J. Chase, Ed.). *Ecology Letters*, *22*(10), 1557–1567. <https://doi.org/10.1111/ele.13345>
- 378
- 379 Barbier, M., & Loreau, M. (2019). Pyramids and cascades: A synthesis of food chain functioning and stability. *Ecology*
380 *Letters*, *22*(2), 405–419. <https://doi.org/10.1111/ele.13196>
- 381 Bennett, A. F., Radford, J. Q., & Haslem, A. (2006). Properties of land mosaics: Implications for nature conservation in
382 agricultural environments. *Biological Conservation*, *133*(2), 250–264. <https://doi.org/10.1016/j.biocon.2006.06.008>
- 383
- 384 Brodie, J. F., Redford, K. H., & Doak, D. F. (2018). Ecological function analysis: Incorporating species roles into conser-
385 vation. *Trends in Ecology & Evolution*, *33*(11), 840–850. <https://doi.org/10.1016/j.tree.2018.08.013>
- 386 Chase, J. M., Jeliakov, A., Ladouceur, E., & Viana, D. S. (2020). Biodiversity conservation through the lens of metacommunity
387 ecology. *Annals of the New York Academy of Sciences*, *1469*(1), 86–104. <https://doi.org/10.1111/nyas.14378>
- 388 Chesson, P. (2000). Mechanisms of maintenance of species diversity. *Annual Review of Ecology and Systematics*, *31*(1),
389 343–366. <https://doi.org/10.1146/annurev.ecolsys.31.1.343>
- 390 Dolson, R., McCann, K., Rooney, N., & Ridgway, M. (2009). Lake morphometry predicts the degree of habitat coupling by
391 a mobile predator. *Oikos*, *118*(8), 1230–1238. <https://doi.org/10.1111/j.1600-0706.2009.17351.x>
- 392 Donadio, E., & Buskirk, S. W. (2016). Linking predation risk, ungulate antipredator responses, and patterns of vegetation
393 in the high Andes. *Journal of Mammalogy*, *97*(3), 966–977. <https://doi.org/10.1093/jmammal/gyw020>
- 394 Economo, E. P. (2011). Biodiversity conservation in metacommunity networks: Linking pattern and persistence. *The Amer-
395 ican Naturalist*, *177*(6), E167–E180. <https://doi.org/10.1086/659946>
- 396 Gehr, B., Bonnot, N. C., Heurich, M., Cagnacci, F., Ciuti, S., Hewison, A. J. M., Gaillard, J.-M., Ranc, N., Premier, J.,
397 Vogt, K., Hofer, E., Ryser, A., Vimercati, E., & Keller, L. (2020). Stay home, stay safe—Site familiarity reduces
398 predation risk in a large herbivore in two contrasting study sites (L. Prugh, Ed.). *Journal of Animal Ecology*,
399 *89*(6), 1329–1339. <https://doi.org/10.1111/1365-2656.13202>

400 Gervasi, V., Sand, H., Zimmermann, B., Mattisson, J., Wabakken, P., & Linnell, J. D. C. (2013). Decomposing risk:
401 Landscape structure and wolf behavior generate different predation patterns in two sympatric ungulates. *Ecological*
402 *Applications*, 23(7), 1722–1734. <https://doi.org/10.1890/12-1615.1>

403 Goldwyn, E. E., & Hastings, A. (2008). When can dispersal synchronize populations? *Theoretical Population Biology*, 73(3),
404 395–402. <https://doi.org/10.1016/j.tpb.2007.11.012>

405 Goldwyn, E. E., & Hastings, A. (2009). Small heterogeneity has large effects on synchronization of ecological oscillators.
406 *Bulletin of Mathematical Biology*, 71(1), 130–144. <https://doi.org/10.1007/s11538-008-9355-9>

407 Gonzalez, A., & Loreau, M. (2008). The causes and consequences of compensatory dynamics in ecological communities.
408 *Annual Review of Ecology, Evolution, and Systematics*, 40(1), 393–414. [https://doi.org/10.1146/annurev.ecolsys.](https://doi.org/10.1146/annurev.ecolsys.39.110707.173349)
409 [39.110707.173349](https://doi.org/10.1146/annurev.ecolsys.39.110707.173349)

410 Gorini, L., Linnell, J. D. C., May, R., Panzacchi, M., Boitani, L., Odden, M., & Nilsen, E. B. (2012). Habitat heterogeneity
411 and mammalian predator-prey interactions: Predator-prey interactions in a spatial world. *Mammal Review*, 42(1),
412 55–77. <https://doi.org/10.1111/j.1365-2907.2011.00189.x>

413 Gravel, D., Massol, F., & Leibold, M. A. (2016). Stability and complexity in model meta-ecosystems. *Nature Communica-*
414 *tions*, 7, 12457. <https://doi.org/10.1038/ncomms12457>

415 Haegeman, B., Arnoldi, J.-F., Wang, S., de Mazancourt, C., Montoya, J. M., & Loreau, M. (2016). Resilience, invariability,
416 and ecological stability across levels of organization. *bioRxiv*. <https://doi.org/10.1101/085852>

417 Hansen, N. A., Sato, C. F., Michael, D. R., Lindenmayer, D. B., & Driscoll, D. A. (2019). Predation risk for reptiles is
418 highest at remnant edges in agricultural landscapes (T. M. Lee, Ed.). *Journal of Applied Ecology*, 56(1), 31–43.
419 <https://doi.org/10.1111/1365-2664.13269>

420 Holt, R. D. (1984). Spatial heterogeneity, indirect interactions, and the coexistence of prey species. *The American Naturalist*,
421 124(3), 377–406. <https://doi.org/10.1086/284280>

422 Holyoak, M., Caspi, T., & Redosh, L. W. (2020). Integrating disturbance, seasonality, multi-year temporal dynamics, and
423 dormancy into the dynamics and conservation of metacommunities. *Frontiers in Ecology and Evolution*, 8, 571130.
424 <https://doi.org/10.3389/fevo.2020.571130>

425 Howeth, J. G., & Leibold, M. A. (2013). Predation inhibits the positive effect of dispersal on intraspecific and interspecific
426 synchrony in pond metacommunities. *Ecology*, 94(10), 2220–2228. <https://doi.org/10.1890/12-2066.1>

427 Jacquet, C., Munoz, F., Bonada, N., Datry, T., Heino, J., & Jabot, F. (2022). Temporal variation of patch connectivity
428 determines biodiversity recovery from recurrent disturbances. *bioRxiv*. <https://doi.org/10.1101/2022.01.02.474736>

429 Jansen, V. A. A. (1999). Phase locking: Another cause of synchronicity in predator–prey systems. *Trends in Ecology &*
430 *Evolution*, 14(7), 278–279. [https://doi.org/10.1016/S0169-5347\(99\)01654-7](https://doi.org/10.1016/S0169-5347(99)01654-7)

431 Jarillo, J., Cao-García, F. J., & De Laender, F. (2022). Spatial and ecological scaling of stability in spatial community
432 networks. *Frontiers in Ecology and Evolution*, 10, 861537. <https://doi.org/10.3389/fevo.2022.861537>

433 Johnson, P. T. J., Hoverman, J. T., McKenzie, V. J., Blaustein, A. R., & Richgels, K. L. D. (2013). Urbanization and wetland
434 communities: Applying metacommunity theory to understand the local and landscape effects (M. Cadotte, Ed.).
435 *Journal of Applied Ecology*, 50(1), 34–42. <https://doi.org/10.1111/1365-2664.12022>

436 Kauffman, M. J., Varley, N., Smith, D. W., Stahler, D. R., MacNulty, D. R., & Boyce, M. S. (2007). Landscape heterogeneity
437 shapes predation in a newly restored predator–prey system. *Ecology Letters*, *10*(8), 690–700. [https://doi.org/10.](https://doi.org/10.1111/j.1461-0248.2007.01059.x)
438 [1111/j.1461-0248.2007.01059.x](https://doi.org/10.1111/j.1461-0248.2007.01059.x)

439 Leibold, M. A., & Chase, J. M. (2017). *Metacommunity Ecology* (Vol. 59). Princeton University Press. [https://doi.org/10.](https://doi.org/10.2307/j.ctt1wf4d24)
440 [2307/j.ctt1wf4d24](https://doi.org/10.2307/j.ctt1wf4d24)

441 Leibold, M. A., Holyoak, M., Mouquet, N., Amarasekare, P., Chase, J. M., Hoopes, M. F., Holt, R. D., Shurin, J. B., Law,
442 R., Tilman, D., Loreau, M., & Gonzalez, A. (2004). The metacommunity concept: A framework for multi-scale
443 community ecology. *Ecology Letters*, *7*(7), 601–613. <https://doi.org/10.1111/j.1461-0248.2004.00608.x>

444 Lloyd, A. L., & May, R. M. (1999). Synchronicity, chaos and population cycles: Spatial coherence in an uncertain world.
445 *Trends in Ecology & Evolution*, *14*(11), 417–418. [https://doi.org/10.1016/S0169-5347\(99\)01717-6](https://doi.org/10.1016/S0169-5347(99)01717-6)

446 Loreau, M., Mouquet, N., & Gonzalez, A. (2003). Biodiversity as spatial insurance in heterogeneous landscapes. *Proceedings*
447 *of the National Academy of Sciences*, *100*(22), 12765–12770. <https://doi.org/10.1073/pnas.2235465100>

448 Loreau, M., & de Mazancourt, C. (2008). Species synchrony and its drivers: Neutral and nonneutral community dynamics
449 in fluctuating environments. *The American Naturalist*, *172*(2), E48–E66. <https://doi.org/10.1086/589746>

450 Loreau, M., & de Mazancourt, C. (2013). Biodiversity and ecosystem stability: A synthesis of underlying mechanisms.
451 *Ecology Letters*, *16*, 106–115. <https://doi.org/10.1111/ele.12073>

452 Lundberg, J., & Moberg, F. (2003). Mobile link organisms and ecosystem functioning: Implications for ecosystem resilience
453 and management. *Ecosystems*, *6*(1), 0087–0098. <https://doi.org/10.1007/s10021-002-0150-4>

454 May, R. M. (1972). Will a large complex system be stable? *Nature*, *238*(5364), 413–414. <https://doi.org/10.1038/238413a0>

455 McCann, K. S., Hastings, A., & Huxel, G. R. (1998). Weak trophic interactions and the balance of nature. *Nature*, *395*(6704),
456 794–798. <https://doi.org/10.1038/27427>

457 Mills, L. S., & Doak, D. F. (1993). The keystone-species concept in ecology and conservation. *BioScience*, *43*(4), 219–224.
458 <https://doi.org/10.2307/1312122>

459 Mouquet, N., Gravel, D., Massol, F., & Calcagno, V. (2013). Extending the concept of keystone species to communities and
460 ecosystems (B. Blasius, Ed.). *Ecology Letters*, *16*(1), 1–8. <https://doi.org/10.1111/ele.12014>

461 Mouquet, N., & Loreau, M. (2002). Coexistence in metacommunities: The regional similarity hypothesis. *The American*
462 *Naturalist*, *159*(4), 420–426. <https://doi.org/10.1086/338996>

463 Mouquet, N., & Loreau, M. (2003). Community patterns in source-sink metacommunities. *The American Naturalist*, *162*(5),
464 544–557. <https://doi.org/10.1086/378857>

465 Mouquet, N., Matthiessen, B., Miller, T., & Gonzalez, A. (2011). Extinction debt in source-sink metacommunities (T.
466 Romanuk, Ed.). *PLoS ONE*, *6*(3), e17567. <https://doi.org/10.1371/journal.pone.0017567>

467 Neutel, A.-M., Heesterbeek, J. A. P., & De Ruiter, P. C. (2002). Stability in real food webs: Weak links in long loops.
468 *Science*, *296*(5570), 1120–1123. <https://doi.org/10.1126/science.1068326>

469 Olf, H., Alonso, D., Berg, M. P., Eriksson, B. K., Loreau, M., Piersma, T., & Rooney, N. (2009). Parallel ecological
470 networks in ecosystems. *Philosophical Transactions of the Royal Society B: Biological Sciences*, *364*(1524), 1755–
471 1779. <https://doi.org/10.1098/rstb.2008.0222>

472 Patrick, C. J., Anderson, K. E., Brown, B. L., Hawkins, C. P., Metcalfe, A., Saffarinia, P., Siqueira, T., Swan, C. M.,
473 Tonkin, J. D., & Yuan, L. L. (2021). The application of metacommunity theory to the management of riverine
474 ecosystems. *WIREs Water*, 8(6). <https://doi.org/10.1002/wat2.1557>

475 Quévreur, P., Barbier, M., & Loreau, M. (2021a). Synchrony and perturbation transmission in trophic metacommunities.
476 *The American Naturalist*, 714131. <https://doi.org/10.1086/714131>

477 Quévreur, P., Pigeault, R., & Loreau, M. (2021b). Predator avoidance and foraging for food shape synchrony and response
478 to perturbations in trophic metacommunities. *Journal of Theoretical Biology*, 528, 110836. <https://doi.org/10.1016/j.jtbi.2021.110836>

480 Rebolo-Ifrán, N., Tella, J. L., & Carrete, M. (2017). Urban conservation hotspots: Predation release allows the grassland-
481 specialist burrowing owl to perform better in the city. *Scientific Reports*, 7(1), 3527. <https://doi.org/10.1038/s41598-017-03853-z>

483 Rooney, N., & McCann, K. S. (2012). Integrating food web diversity, structure and stability. *Trends in Ecology & Evolution*,
484 27(1), 40–46. <https://doi.org/10.1016/j.tree.2011.09.001>

485 Rooney, N., McCann, K. S., Gellner, G., & Moore, J. C. (2006). Structural asymmetry and the stability of diverse food
486 webs. *Nature*, 442(7100), 265–269. <https://doi.org/10.1038/nature04887>

487 Ruokolainen, L., Abrams, P. A., McCann, K. S., & Shuter, B. J. (2011). The roles of spatial heterogeneity and adaptive
488 movement in stabilizing (or destabilizing) simple metacommunities. *Journal of Theoretical Biology*, 291, 76–87.
489 <https://doi.org/10.1016/j.jtbi.2011.09.004>

490 Schindler, D. E., & Scheuerell, M. D. (2002). Habitat coupling in lake ecosystems. *Oikos*, 98(2), 177–189. <https://doi.org/10.1034/j.1600-0706.2002.980201.x>

492 Shochat, E., Warren, P., Faeth, S., McIntyre, N., & Hope, D. (2006). From patterns to emerging processes in mechanistic
493 urban ecology. *Trends in Ecology & Evolution*, 21(4), 186–191. <https://doi.org/10.1016/j.tree.2005.11.019>

494 Shochat, E., Lerman, S. B., Anderies, J. M., Warren, P. S., Faeth, S. H., & Nilon, C. H. (2010). Invasion, competition, and
495 biodiversity loss in urban ecosystems. *BioScience*, 60(3), 199–208. <https://doi.org/10.1525/bio.2010.60.3.6>

496 Soulé, M. E., Estes, J. A., Miller, B., & Honnold, D. L. (2005). Strongly interacting species: Conservation policy, manage-
497 ment, and ethics. *BioScience*, 55(2), 168. [https://doi.org/10.1641/0006-3568\(2005\)055\[0168:SISCPM\]2.0.CO;2](https://doi.org/10.1641/0006-3568(2005)055[0168:SISCPM]2.0.CO;2)

498 Thaker, M., Vanak, A. T., Owen, C. R., Ogden, M. B., Niemann, S. M., & Slotow, R. (2011). Minimizing predation risk in a
499 landscape of multiple predators: Effects on the spatial distribution of African ungulates. *Ecology*, 92(2), 398–407.
500 <https://doi.org/10.1890/10-0126.1>

501 Vadeboncoeur, Y., McCann, K. S., Zanden, M. J. V., & Rasmussen, J. B. (2005). Effects of multi-chain omnivory on the
502 strength of trophic control in lakes. *Ecosystems*, 8(6), 682–693. <https://doi.org/10.1007/s10021-003-0149-5>

503 Van Teeffelen, A. J., Vos, C. C., & Opdam, P. (2012). Species in a dynamic world: Consequences of habitat network dynamics
504 on conservation planning. *Biological Conservation*, 153, 239–253. <https://doi.org/10.1016/j.biocon.2012.05.001>

505 Vasseur, D. A., & Fox, J. W. (2009). Phase-locking and environmental fluctuations generate synchrony in a predator–prey
506 community. *Nature*, 460(7258), 1007–1010. <https://doi.org/10.1038/nature08208>

507 Wang, S., Haegeman, B., & Loreau, M. (2015). Dispersal and metapopulation stability. *PeerJ*, 3, e1295. <https://doi.org/10.7717/peerj.1295>

508

- 509 Wang, S., Lamy, T., Hallett, L. M., & Loreau, M. (2019). Stability and synchrony across ecological hierarchies in heteroge-
510 neous metacommunities: Linking theory to data. *Ecography*, *0*(0). <https://doi.org/10.1111/ecog.04290>
- 511 Wang, S., & Loreau, M. (2014). Ecosystem stability in space: α , β and γ variability. *Ecology*
512 *Letters*, *17*(8), 891–901. <https://doi.org/10.1111/ele.12292>
- 513 Wang, S., & Loreau, M. (2016). Biodiversity and ecosystem stability across scales in metacommunities (F. Jordan, Ed.).
514 *Ecology Letters*, *19*(5), 510–518. <https://doi.org/10.1111/ele.12582>
- 515 Wilcox, K. R., Tredennick, A. T., Koerner, S. E., Grman, E., Hallett, L. M., Avolio, M. L., Pierre, K. J. L., Houseman, G. R.,
516 Isbell, F., Johnson, D. S., Alatalo, J. M., Baldwin, A. H., Bork, E. W., Boughton, E. H., Bowman, W. D., Britton,
517 A. J., Cahill, J. F., Collins, S. L., Du, G., . . . Zhang, Y. (2017). Asynchrony among local communities stabilises
518 ecosystem function of metacommunities. *Ecology Letters*, *20*(12), 1534–1545. <https://doi.org/10.1111/ele.12861>

519 S1 Complementary material and methods

520 S1-1 Model description

The model has been originally developed by Barbier and Loreau (2019), who considered a food chain model with a simple metabolic parametrisation. Their model corresponds to the "intra-patch dynamics" part of equations (5a) and (5b) to which we graft a dispersal term to consider a metacommunity with two patches.

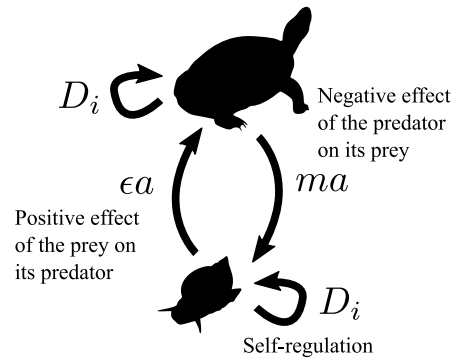
$$\frac{dB_1^{(1)}}{dt} = B_1^{(1)}(\omega_1 g_1 - D_1 B_1^{(1)} - \gamma_1 \alpha_{2,1} B_2^{(1)}) + \delta_1 (B_1^{(2)} - B_1^{(1)}) \quad (5a)$$

$$\frac{dB_i^{(1)}}{dt} = \underbrace{B_i^{(1)}(-r_i - D_i B_i^{(1)} + \gamma_1 \epsilon \alpha_{i,i-1} B_{i-1}^{(1)} - \gamma_1 \alpha_{i+1,i} B_{i+1}^{(1)})}_{\text{intra-patch dynamics}} + \underbrace{\delta_i (B_i^{(2)} - B_i^{(1)})}_{\text{dispersal}} \quad (5b)$$

521 $B_i^{(1)}$ is the biomass of trophic level i in the patch #1, ϵ is the biomass conversion efficiency and $\alpha_{i,j}$ is the
 522 interaction strength between consumer i and prey j . Species i disperses between the two patches at rate
 523 δ_i . The density independent net growth rate of primary producers g_i in equations (5a), the mortality
 524 rate of consumers r_i in equations (5b) and the density dependent mortality rate D_i scale with species
 525 metabolic rates m_i as biological rates are linked to energy expenditure.

$$g_1 = m_1 g \quad r_i = m_i r \quad D_i = m_i D \quad (6)$$

In order to get a broad range of possible responses, we assume the predator-prey metabolic rate ratio m and the interaction strength to self-regulation ratio a to be constant. These ratios
 526 capture the relations between parameters and trophic levels. This enables us to consider contrasting situations while keeping the model as simple as possible.



$$m = \frac{m_{i+1}}{m_i} \quad a = \frac{\alpha_{i,i-1}}{D_i} \quad d_i = \frac{\delta_i}{D_i} \quad (7)$$

Varying m leads to food chains where predators have faster or slower biomass dynamics than their prey and varying a leads to food chains where interspecific interactions prevail or not compared with intraspecific interactions. As all biological rates are rescaled by D_i , we also define d_i , the dispersal rate relative to self-regulation (referred as scaled dispersal rate in the rest of the study), in order to keep the

values of the dispersal rate relative to the other biological rates consistent across trophic levels. Finally, the time scale of the system is defined by setting the metabolic rate of the primary producer m_1 to unity. Thus, we can transform equations (5a) and (5b) into:

$$\frac{1}{D} \frac{dB_1^{(1)}}{dt} = B_1^{(1)} \left(\omega \frac{g}{D} - B_1^{(1)} - \gamma ma B_2^{(1)} \right) + d_1 (B_1^{(2)} - B_1^{(1)}) \quad (8a)$$

$$\frac{1}{m^{i-1}D} \frac{dB_i^{(1)}}{dt} = \underbrace{B_i^{(1)} \left(-\frac{r}{D} - B_i^{(1)} + \gamma \epsilon a B_{i-1}^{(1)} - \gamma ma B_{i+1}^{(1)} \right)}_{\text{intra-patch dynamics}} + \underbrace{d_i (B_i^{(2)} - B_i^{(1)})}_{\text{dispersal}} \quad (8b)$$

527 Thus, ϵa and ma defines the positive effect of the prey on its predator and the negative effect of the
 528 predator on its prey, respectively. These two synthetic parameters define the overall behaviour of the
 529 food chain and will be varied over the interval $[0.1, 10]$ to consider a broad range of possible responses.

530 **S1-2 Biomass at equilibrium when top predators populations are perfectly** 531 **coupled**

The system can be easily solved if we consider the total population of top predator instead of two populations connected by dispersal. Since the two populations are perfectly coupled by dispersal, top predator i biomass is constant across patches and we have $B_i^{(1)*} = B_i^{(2)*} = 0.5 B_i^{*tot}$. Thus we have the following system at equilibrium for the two top species (the equations for the other species are the same as the symmetric case):

$$0 = -\frac{r}{D} - B_i^{*tot} + \epsilon a \left(\gamma B_{i-1}^{*(1)} + B_{i-1}^{*(2)} \right) \quad (9a)$$

$$0 = -\frac{r}{D} - B_{i-1}^{*(1)} + \gamma \epsilon a B_{i-2}^{*(1)} - \gamma ma \frac{B_i^{*tot}}{2} \quad (9b)$$

$$0 = -\frac{r}{D} - B_{i-1}^{*(2)} + \epsilon a B_{i-2}^{*(2)} - ma \frac{B_i^{*tot}}{2} \quad (9c)$$

534 **S1-4 Linearisation of the system**

The system of equations (1a) and (1b) can be linearised in the vicinity of equilibrium:

$$\frac{dB_i}{dt} = \underbrace{f_i(B_1^*, \dots, B_S^*)}_{=0} + \sum_{j=1}^S \left(\left. \frac{\partial f_i}{\partial B_j} \right|_{B^*} (B_j - B_j^*) \right) \quad (13)$$

Thus, by setting $X_i = B_i - B_i^*$ the deviation from equilibrium, we have:

$$\frac{dX_i}{dt} = \sum_{j=1}^S J_{ij} X_j \quad (14)$$

Then, we can consider small perturbations defined by \vec{E} whose effects on \vec{X} are defined by the matrix T (Arnoldi et al., 2016). We get the linearised version of equation (2):

$$\frac{d\vec{X}}{dt} = J\vec{X} + T\vec{E} \quad (15)$$

535 The elements of \vec{E} are defined by stochastic perturbations $E_i = \sigma_i dW_i$ with σ_i their standard deviation
 536 and dW_i a white noise term with mean 0 and variance 1. In our model, each species i in each patch k can
 537 receive demographic perturbations scaling with the square root of their biomass at equilibrium. Thus,
 538 \vec{E} contains the white noise term $\sigma_i^{(k)} dW_i^{(k)}$ for each population of each species, T is a diagonal matrix
 539 whose terms are $\sqrt{B_i^{*(k)}}$ and the matrix product $T\vec{E}$ results in the product of the white noise and the
 540 biomass scaling as in equation (2) in the main text.

541 **S1-5 Resolution of the Lyapunov equation**

In the vicinity of equilibrium, the Lyapunov equation links the variance-covariance matrix V_E of the perturbation vector \vec{E} to the variance-covariance matrix C^* of species biomasses (see the appendix of Wang et al. (2015) for more details on the Lyapunov equation).

$$JC^* + C^*J^\top + TV_E T^\top = 0 \quad (16)$$

The diagonal elements of V_E are equal to σ_i^2 (variance of the white noises) and the non-diagonal elements are equal to zero because perturbations are independent. \top is the transpose operator. C^* can be calculated using a Kronecker product (Nip et al., 2013). The Kronecker product of an $m \times n$ matrix A

and a $p \times q$ matrix B denoted $A \otimes B$ is the $mp \times nq$ block matrix given by:

$$A \otimes B = \begin{pmatrix} a_{11}B & \cdots & a_{1n}B \\ \vdots & \ddots & \vdots \\ a_{m1}B & \cdots & a_{mn}B \end{pmatrix}$$

We define C_s^* and $(TV_E T^\top)_s$ the vectors stacking the columns of C^* and $TV_E T^\top$ respectively. Thus, equation (16) can be rewrite as:

$$\begin{aligned} (J \otimes I + I \otimes J)C_s^* &= -(TV_E T^\top)_s \\ C_s^* &= -(J \otimes I + I \otimes J)^{-1}(TV_E T^\top)_s \end{aligned} \quad (17)$$

542 S1-6 Coefficient of variation and correlation

Our different metrics of stability can be easily computed from the elements of the variance-covariance matrix C^* defined by elements $w_{i^{(k)}j^{(\ell)}}$ that are the covariance between species i in patch k and species j in patch ℓ .

$$C^* = \begin{pmatrix} w_{1^{(1)}1^{(1)}} & \cdots & w_{1^{(1)}S^{(1)}} & \cdots & w_{1^{(n)}1^{(n)}} & \cdots & w_{1^{(n)}S^{(n)}} \\ \vdots & \ddots & \vdots & \cdots & \vdots & \ddots & \vdots \\ w_{S^{(1)}1^{(1)}} & \cdots & w_{S^{(1)}S^{(1)}} & \cdots & w_{S^{(n)}1^{(n)}} & \cdots & w_{S^{(n)}S^{(n)}} \\ \vdots & \vdots & \vdots & \ddots & \vdots & \vdots & \vdots \\ w_{1^{(n)}1^{(1)}} & \cdots & w_{1^{(n)}S^{(1)}} & \cdots & w_{1^{(n)}1^{(n)}} & \cdots & w_{1^{(n)}S^{(n)}} \\ \vdots & \ddots & \vdots & \cdots & \vdots & \ddots & \vdots \\ w_{S^{(n)}1^{(1)}} & \cdots & w_{S^{(n)}S^{(1)}} & \cdots & w_{S^{(n)}1^{(n)}} & \cdots & w_{S^{(n)}S^{(n)}} \end{pmatrix} \quad (18)$$

The temporal variability of the metacommunity is assessed with the coefficient of variation (CV) of biomass at different scales: **population scale** $CV_i^{(k)}$, which is the biomass CV of species i in patch k , **metapopulation scale** CV_i , which is the biomass CV of the total biomass of species i across patches and **metacommunity scale** CV_{MC} , which is the total biomass of the entire metacommunity (Wang and Loreau, 2014; Wang et al., 2019; Jarillo et al., 2022).

$$CV_i^{(k)} = \frac{\sqrt{w_{i^{(k)}i^{(k)}}}}{\mu_i^{(k)}} \quad CV_i = \frac{\sqrt{\sum_{k\ell} w_{i^{(k)}j^{(\ell)}}}}{\sum_k B_i^{*(k)}} \quad CV_{MC} = \frac{\sqrt{\sum_{ijk\ell} w_{i^{(k)}j^{(\ell)}}}}{\sum_{ik} B_i^{*(k)}} \quad (19)$$

$$C^* = \begin{pmatrix}
w_{1(1)1(1)} \cdots w_{1(1)S(1)} \cdots w_{1(n)1(n)} \cdots w_{1(n)S(n)} & & & & \\
\vdots & \ddots & \vdots & \cdots & \vdots & \ddots & \vdots \\
w_{S(1)1(1)} \cdots w_{S(1)S(1)} \cdots w_{S(n)1(n)} \cdots w_{S(n)S(n)} & & & & \\
\vdots & \vdots & \vdots & \ddots & \vdots & \vdots & \vdots \\
w_{1(n)1(1)} \cdots w_{1(n)S(1)} \cdots w_{1(n)1(n)} \cdots w_{1(n)S(n)} & & & & \\
\vdots & \vdots & \vdots & \ddots & \vdots & \vdots & \vdots \\
w_{S(n)1(1)} \cdots w_{S(n)S(1)} \cdots w_{S(n)1(n)} \cdots w_{S(n)S(n)} & & & &
\end{pmatrix}$$

$CV_i^{(k)}$
 CV_i
 CV_{MC}

Figure S1-1: Elements of the variance-covariance matrix C^* used to compute the biomass CV at different scales defined in equation (19).

The correlation matrix R^* of the system, whose elements $\rho_{i^{(k)}j^{(\ell)}}$ are defined by:

$$\rho_{i^{(k)}j^{(\ell)}} = \frac{w_{i^{(k)}j^{(\ell)}}}{\sqrt{w_{i^{(k)}i^{(k)}}} \sqrt{w_{j^{(\ell)}j^{(\ell)}}}} \tag{20}$$

543 S1-7 Asymptotic resilience

544 In addition to the response to stochastic perturbations, we consider asymptotic resilience to measure
545 the long term return time of the metacommunity. Asymptotic resilience is measured by the opposite of
546 the real part of the dominant eigenvalue λ_{dom} of Jacobian matrix J ($-\Re(\lambda_{dom})$). Since the dominant
547 eigenvalue is the eigenvalue with the largest real part and we only consider ecosystems at equilibrium
548 (*i.e.* all eigenvalues have negative real parts), the lower the real part of the dominant eigenvalue, the
549 faster the long term return time.

550 Moreover, we can assess the influence of each species on asymptotic resilience by comparing the absolute
551 value of the real part of each element e_i of the dominant eigenvector (E_{dom}). Because e_i is the contribution
552 of species i to E_{dom} , $|e_i| / \sum_{j=1}^n |e_j|$ is the relative weight of species i in the dynamics of long term return
553 to equilibrium (with n the number of populations in the metacommunity).

554 References

- 555 Arnoldi, J.-F., Loreau, M., & Haegeman, B. (2016). Resilience, reactivity and variability: A mathematical comparison of
556 ecological stability measures. *Journal of Theoretical Biology*, 389, 47–59. <https://doi.org/10.1016/j.jtbi.2015.10.012>
557
558 Barbier, M., & Loreau, M. (2019). Pyramids and cascades: A synthesis of food chain functioning and stability. *Ecology*
559 *Letters*, 22(2), 405–419. <https://doi.org/10.1111/ele.13196>

- 560 Jarillo, J., Cao-García, F. J., & De Laender, F. (2022). Spatial and ecological scaling of stability in spatial community
561 networks. *Frontiers in Ecology and Evolution*, *10*, 861537. <https://doi.org/10.3389/fevo.2022.861537>
- 562 Nip, M., Hespanha, J. P., & Khammash, M. (2013). Direct numerical solution of algebraic Lyapunov equations for large-
563 scale systems using Quantized Tensor Trains. *52nd IEEE Conference on Decision and Control*, 1950–1957. <https://doi.org/10.1109/CDC.2013.6760167>
- 564
- 565 Wang, S., Haegeman, B., & Loreau, M. (2015). Dispersal and metapopulation stability. *PeerJ*, *3*, e1295. <https://doi.org/10.7717/peerj.1295>
- 566
- 567 Wang, S., Lamy, T., Hallett, L. M., & Loreau, M. (2019). Stability and synchrony across ecological hierarchies in heteroge-
568 neous metacommunities: Linking theory to data. *Ecography*, *0*(0). <https://doi.org/10.1111/ecog.04290>
- 569 Wang, S., & Loreau, M. (2014). Ecosystem stability in space: α , β and γ variability. *Ecology*
570 *Letters*, *17*(8), 891–901. <https://doi.org/10.1111/ele.12292>

571 **S2 Complementary results**

572 **S2-1 General description of parameters**

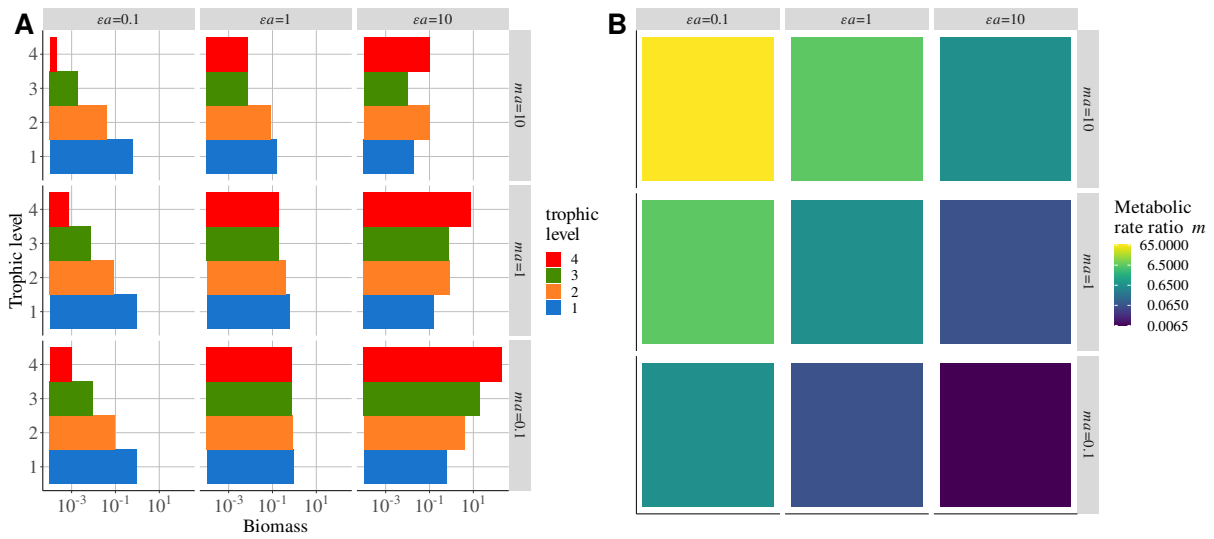


Figure S2-1: Distribution of parameters and their effects on an isolated food chain. **A)** Biomass distribution depending on the positive effect of prey on predator ϵa and the negative effect of predator on prey $m a$. **B)** Value of the ratio of predator to prey metabolic rate $m = m_{i+1}/m_i$ for each combination of ϵa and $m a$.

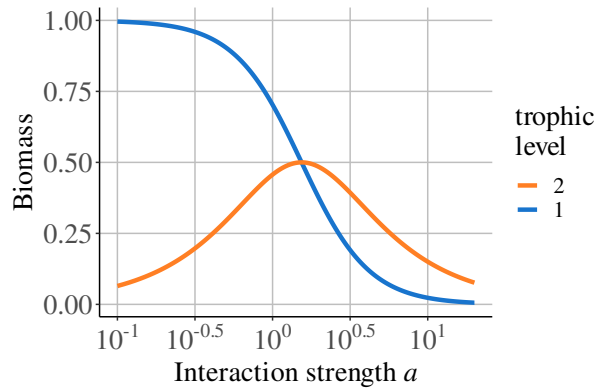


Figure S2-2: Distribution of biomass in an isolated predator-prey system (without dispersal) depending on interaction strength a relative to self-regulation. Increasing the asymmetry of the interaction strength γ is equivalent to increasing a ($m = 0.65$).

573 Increasing the interaction strength a relative to self-regulation decreases the biomass of prey because
 574 of the increased mortality due to predation (Figure S2-2). However, the biomass of predators follows a
 575 hump-shaped relationship: it first increases due to the increased resource consumption and then decreases
 576 because of prey overexploitation.

577 **S2-2 Dispersal of predators and perturbation of prey**

578 **S2-2-1 Conditions of coexistence**

579 Asymmetry and dispersal lead to competition, apparent competition and source-sink dynamics that
 580 can rescue or drive local populations to extinction. Therefore, we consider limit cases in which dispersal
 581 is infinite (well mixed populations across the metacommunity) to analytically calculate biomasses at
 582 equilibrium and determine the range of values of ω and γ enabling the coexistence of all populations of
 583 each species.

We consider the total biomass of predators $B_2^{tot} = B_2^{(1)} + B_2^{(2)}$ and because the very high dispersal of predators equally distributes its biomass among the two patches, we have $B_2^{*tot} = 2 \times B_2^{*(1)}$. Then, we can define the system:

$$\frac{dB_1^{(1)}}{dt} = DB_1^{(1)} \left(\frac{\omega g}{D} - B_1^{(1)} - \gamma ma \frac{B_2^{tot}}{2} \right) \quad (21a)$$

$$\frac{dB_1^{(2)}}{dt} = DB_1^{(2)} \left(\frac{g}{D} - B_1^{(2)} - ma \frac{B_2^{tot}}{2} \right) \quad (21b)$$

$$\frac{dB_2^{tot}}{dt} = mD \frac{B_2^{tot}}{2} \left(-\frac{r}{D} - B_2^{tot} + \varepsilon a (\gamma B_1^{(1)} + B_1^{(2)}) \right) \quad (21c)$$

Since $r = 0$, we remove it from the equations for the sake of simplicity. We define $\lambda = \varepsilon ma^2$, which is the intensity of top-down control defined by Barbier and Loreau (2019). At equilibrium, we obtain:

$$B_1^{(1)*} = \frac{g}{D} \left(\frac{2\omega + \omega\lambda - \gamma\lambda}{2 + \lambda(\gamma^2 + 1)} \right) \quad (22a)$$

$$B_1^{(2)*} = \frac{g}{D} \left(\frac{\lambda\gamma^2 - \omega\lambda\gamma + 2}{2 + \lambda(\gamma^2 + 1)} \right) \quad (22b)$$

$$B_2^{tot*} = \frac{2\varepsilon ag(1 + \omega\gamma)}{D(2 + \varepsilon a^2 m(\gamma^2 + 1))} \quad (22c)$$

Prey biomass in patch #1 $B_1^{*(1)}$ is positive only if:

$$\gamma < \frac{\omega(2 + \lambda)}{\lambda} \xrightarrow{\lambda \rightarrow \infty} \omega \quad (23)$$

Prey biomass in patch #2 $B_1^{*(2)}$ is positive if $f(\gamma) = \lambda\gamma^2 - \omega\lambda\gamma + 2 > 0$. f opens upwards: thus, if

$\omega < \sqrt{8/\lambda}$, f has no roots and is always positive. Otherwise, $B_1^{(2)}$ is positive if:

$$\gamma > \frac{\lambda\omega + \sqrt{\lambda(\lambda\omega^2 - 8)}}{2\lambda} \xrightarrow{\lambda \rightarrow \infty} \omega \quad \text{if } \omega > \sqrt{\frac{8}{\lambda}} \quad \text{or} \quad (24a)$$

$$\gamma < \frac{\lambda\omega - \sqrt{\lambda(\lambda\omega^2 - 8)}}{2\lambda} \xrightarrow{\lambda \rightarrow \infty} 0 \quad \text{if } \omega > \sqrt{\frac{8}{\lambda}} \quad (24b)$$

584 Predators B_2 thrive in each patch for all values of ω and γ (Figure S2-3C). Hence, coexistence is ensured for
 585 all values of top-down control λ , asymmetry of resource supply ω and asymmetry of interaction strength
 586 γ only if $\gamma = \omega$. In the main text, we always consider $\gamma = \omega$ (Figure S2-3D), but their independent effects
 587 are detailed in the following.

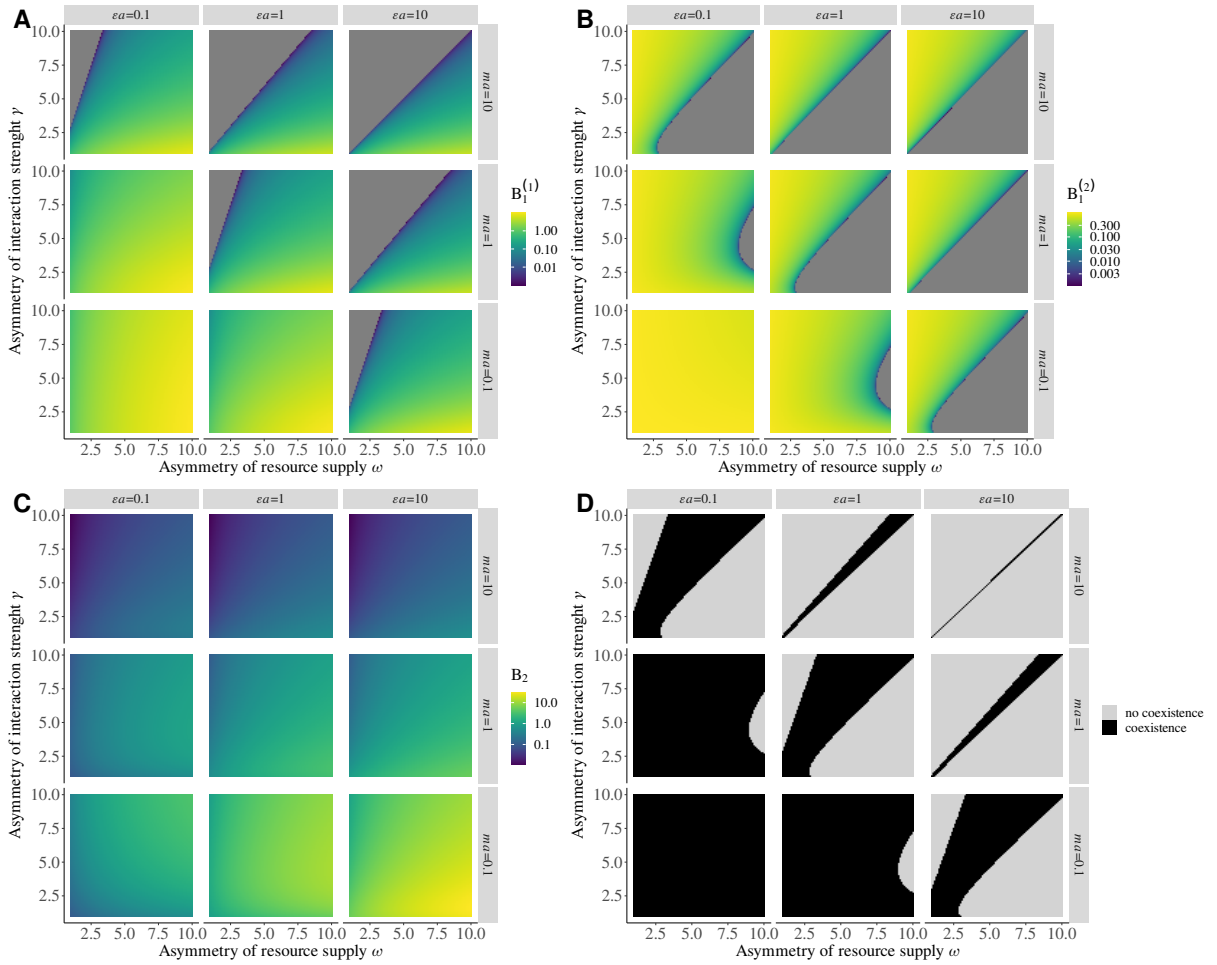


Figure S2-3: Distribution of parameters, asymmetry of resource supply ω and asymmetry of interaction strength γ , leading to the coexistence of predator and prey in each patch. Only predators are able to disperse at an infinite rate (well-mixed predator populations). This distribution is assessed for different values of the positive effect of prey on predator ϵa and negative effect of predator on prey ma . **A)** Biomass of prey in patch #1 $B_1^{*(1)}$ and **B)** in patch #2 $B_1^{*(2)}$. **C)** Biomass of predator in patches #1 and #2 ($B_2^{*(1)} = B_2^{*(2)}$ because predator populations are well mixed). **D)** Coexistence of predator and prey in each patch.

588 **S2-2-2 Nontransitivity of correlation**

589 To explain the correlation between prey populations, we can track the transmission of perturbations in
 590 the metacommunity. Increasing the asymmetry of interaction strength γ tends to decorrelate predator and
 591 prey dynamics within each patch (Figure S2-4A). When prey are perturbed in patch #1, the dynamics
 592 of predator and prey biomass are correlated in patch #1 and anticorrelated in patch #2 due to the
 593 bottom-up and top-down transmissions of perturbations, respectively. Although we would expect the
 594 two populations of prey to be anti-correlated according to the mechanism described by Quévieux et al.
 595 (2021) (see Figure S2-25 in the following), we actually observe a weak correlation of these two populations
 596 (Figure S2-4B). In the same way, the intermediate correlation and anti-correlation of predator and prey
 597 when prey are perturbed in patch #2 do not explain the strong anti-correlation of prey populations
 598 (Figure S2-4C). Therefore, other mechanisms are acting in our system.

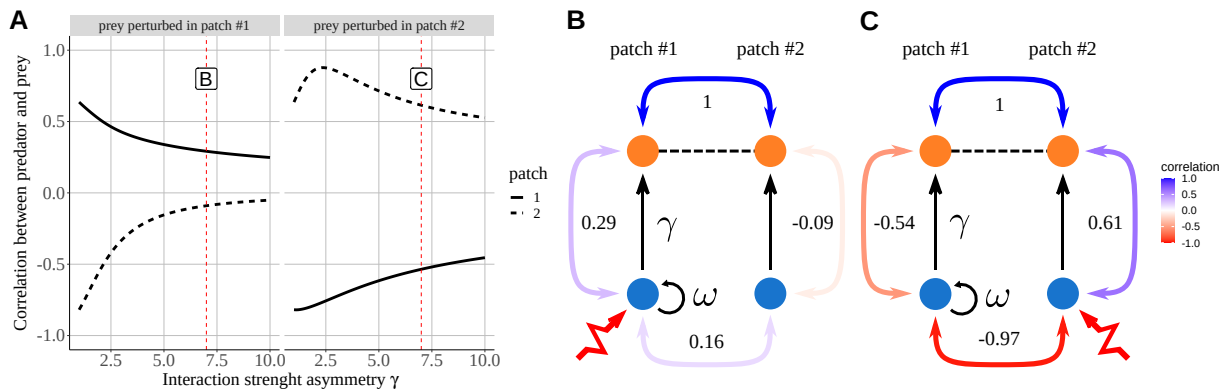


Figure S2-4: Correlation between predator and prey with each patch ($\varepsilon a = 1$, $ma = 1$, $d_2 = 10^6$, $\omega = \gamma$). **A)** Correlation in each patch depending on asymmetry of interaction strength γ when prey in patch #1 (left panel) or in patch #2 (right panel) are perturbed. Labels and vertical dashed lines represent the correlation values used in panels B and C. **B)** Schematic representation of correlations when $\gamma = 7$. Coloured double arrows and their associated number (see also the colour scale) represent the correlations between populations. Prey are perturbed in patch #1. **C)** Prey are perturbed in patch #2.

599 **S2-2-3 Complete effects of εa and ma**

600 The stability patterns observed in Figures 3 to 5 in the main text are also observed for a wide range of
 601 ecological and physiological parameters aggregated into the positive effect of prey on predators εa and the
 602 negative effect on predators on prey ma . Therefore, our results are robust and the identified mechanisms
 603 are specific to a particular combination of parameters.

604 The response of the asymptotic resilience to the asymmetry of interaction strength (Figure S2-8A)
 605 is not similar to the results of Rooney et al. (2006). Indeed, we do not observe minimum of resilience
 606 for $\gamma = 1$ for all combinations of εa and ma . The variations in asymptotic resilience depend on the

607 relative contribution of each population of each species (Figure S2-8B), which is governed by the biomass
 608 distribution of each species among patches (Figure S2-5A) and the ratio of predator to prey metabolic
 609 rate ratio m (Figure S2-1B). As demonstrated by Haegeman et al. (2016) and Arnoldi et al. (2018),
 610 rare species control the long term recovery to perturbations of the metacommunity (*i.e.*, the asymptotic
 611 resilience), as well as species with a slow pace of life (*i.e.*, a slow metabolism).

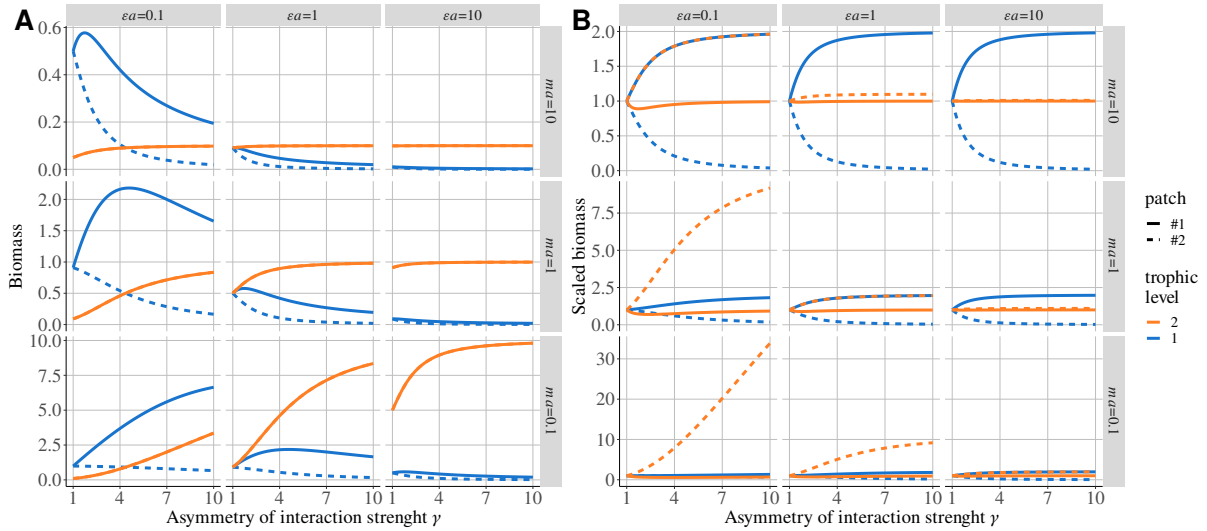


Figure S2-5: Biomass distribution of each species in each patch depending on asymmetry of interaction strength γ , positive effect of prey on predator ϵa and negative effect of predator on prey $m a$. **A)** Biomass distribution. **B)** Biomass scaled by the biomass in the metacommunity without dispersal ($d_2 = 0$).

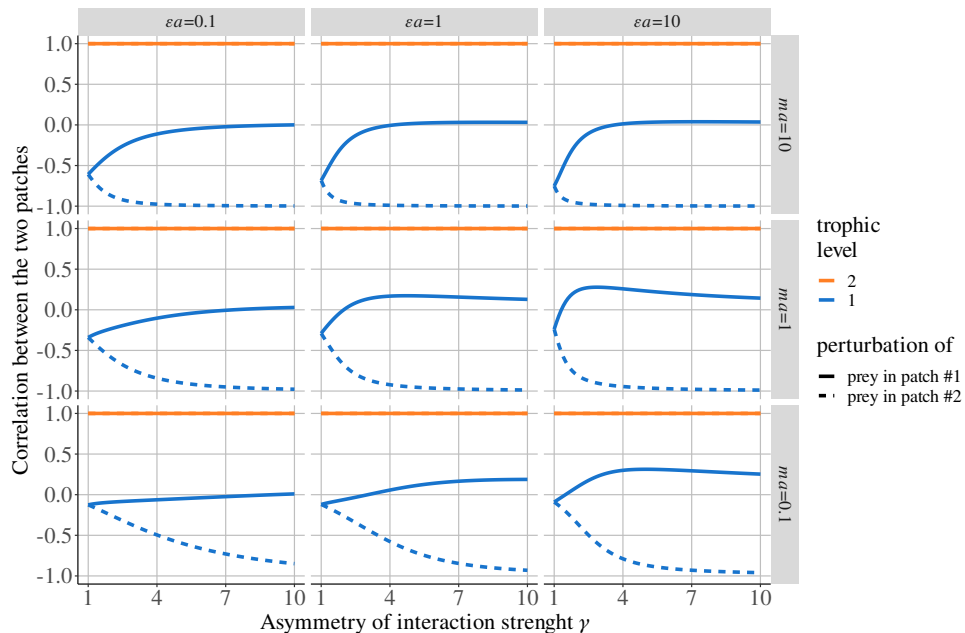


Figure S2-6: Correlation between populations depending on asymmetry in interaction strength γ when predators disperse and prey are perturbed in patch #1 or #2. Predators have a high scaled dispersal rate ($d_2 = 10^6$), which strongly couples their two populations ($\gamma = \omega$).

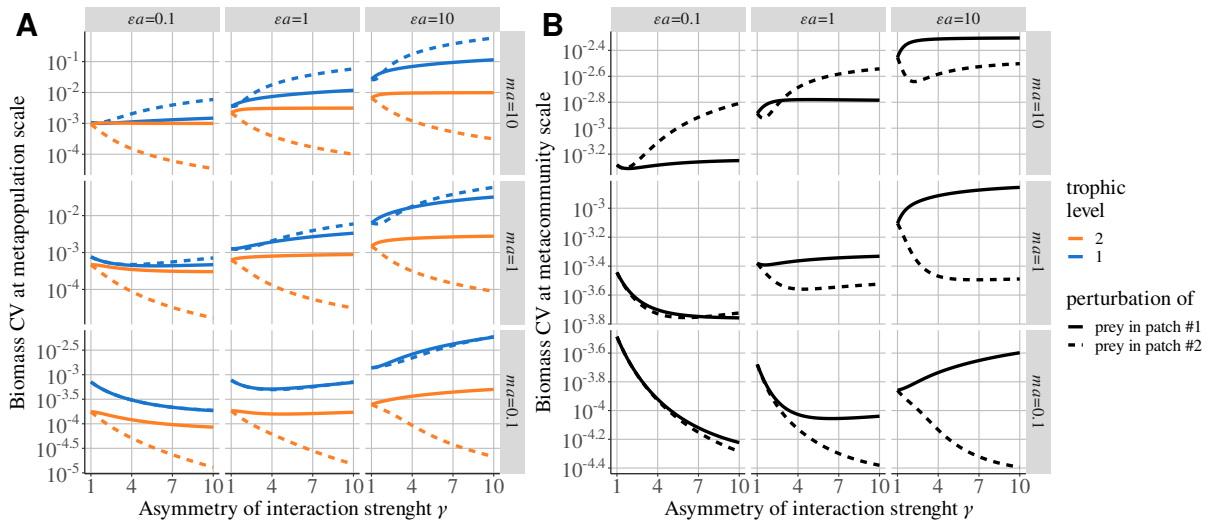


Figure S2-7: Biomass CV at different scales depending on asymmetry of interaction strength γ , positive effect of prey on predator ϵa and negative effect of predator on prey ma ($d_2 = 10^6$ and $\omega = \gamma$). **A**) Biomass CV of the population of each species in each patch. **B**) CV of the total biomass of each species.

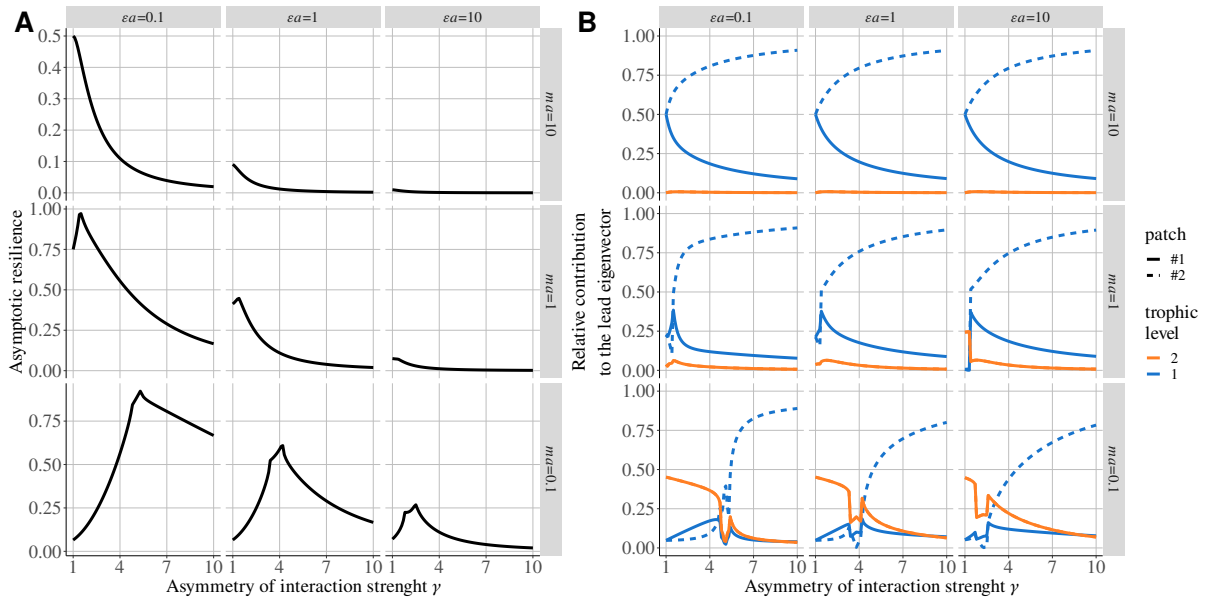


Figure S2-8: Linear stability depending on asymmetry of interaction strength γ , positive effect of prey on predator ϵa and negative effect of predator on prey ma . **A**) Asymptotic resilience (real part of the dominant eigenvalue of the Jacobian matrix) **B**) Contribution of the populations of each species to the dominant eigenvector.

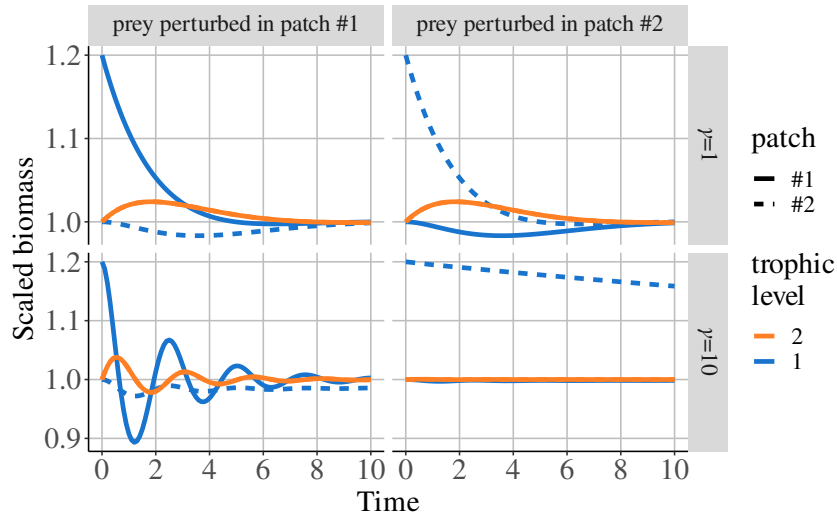


Figure S2-9: Time series of biomasses rescaled by their value at equilibrium after an increase in prey biomass by 20% in patch #1 (left panel) or patch #2 (right panel) for two values of interaction strength asymmetry ($\gamma = 1$ or $\gamma = 10$, $\epsilon a = 1$, $m a = 1$, $d_2 = 10^6$ and $\omega = \gamma$).

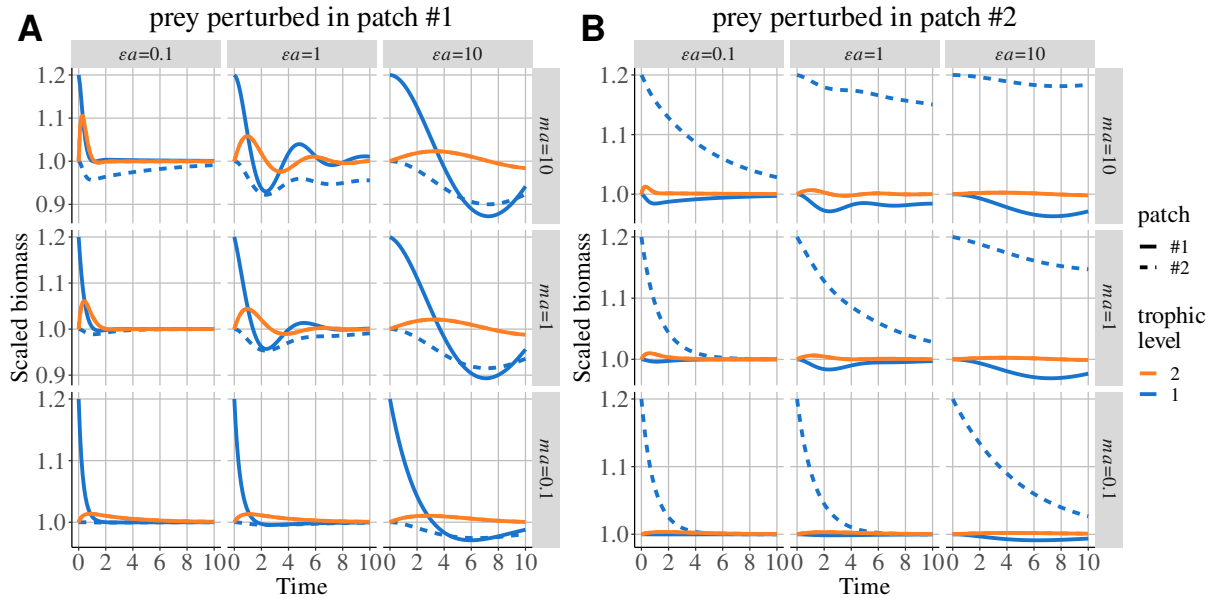


Figure S2-10: Time series of biomasses rescaled by their value at equilibrium after an increase in prey biomass by 20% in patch #1 (left panel) or patch #2 (right panel) depending on asymmetry of interaction strength γ , positive effect of prey on predator ϵa and negative effect of predator on prey $m a$ ($\gamma = 3$, $d_2 = 10^6$ and $\omega = \gamma$).

612 S2-2-4 Effect of asymmetry of resource supply ω

613 According to Figure S2-3, we set $\omega = \gamma$ to ensure the coexistence of prey and predators in each patch for
 614 all combinations of ϵa and $m a$. Varying the asymmetry of resource supply ω does not qualitatively alter
 615 the response of biomass (Figure S2-11), correlation (Figure S2-12A) and biomass CV (Figure S2-12B) to
 616 the variations in the asymmetry of interaction strength γ .

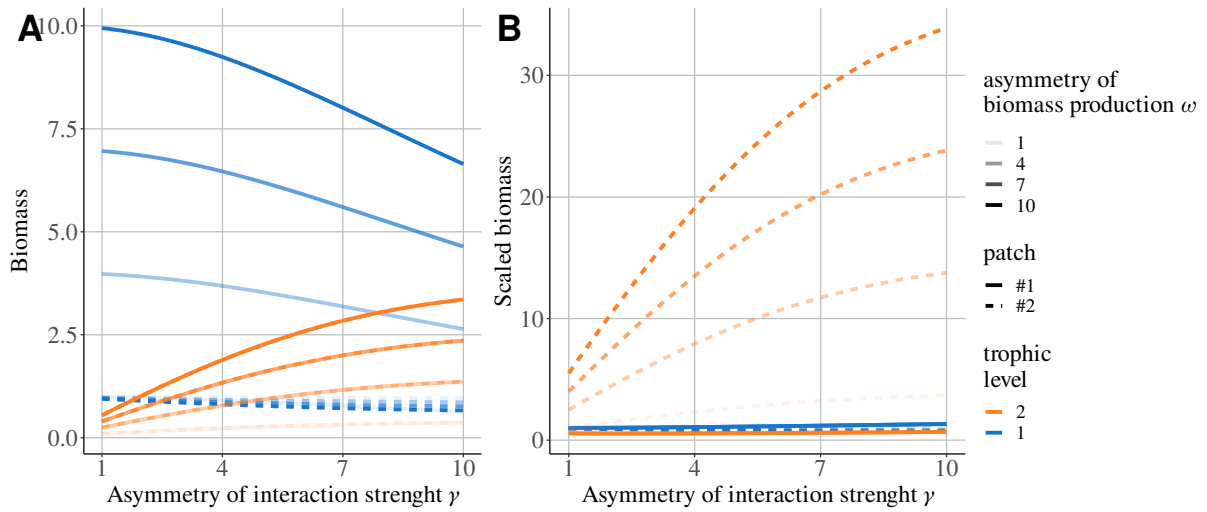


Figure S2-11: Biomass distribution of each species in each patch depending on asymmetry of interaction strength γ and biomass production ω ($\epsilon a = 0.1$, $ma = 0.1$ and $d_2 = 10^6$). **A**) Biomass distribution. **B**) Biomass scaled by the biomass in the metacommunity without dispersal ($d_2 = 0$).

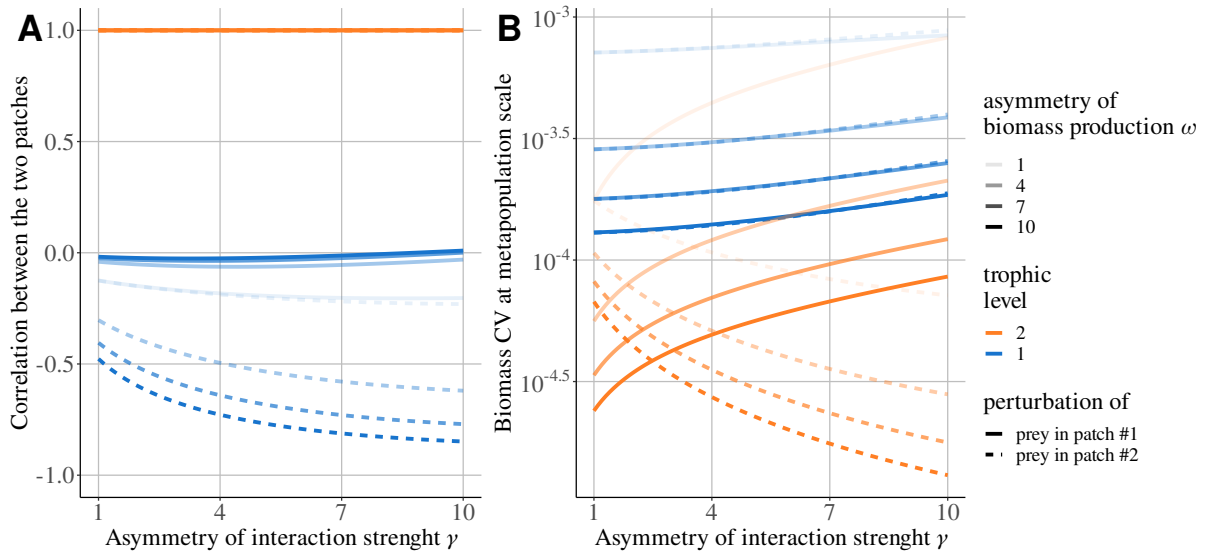


Figure S2-12: Stability depending on asymmetry of interaction strength γ and biomass production ω ($\epsilon a = 0.1$, $ma = 0.1$ and $d_2 = 10^6$). **A**) Correlation between populations. **B**) Biomass CV of the population of each species in each patch.

617 S2-2-5 Effect of perturbation of predators

618 The perturbation of predators leads to the same response regardless of the perturbed patch because
 619 the very high dispersal of predators perfectly synchronises their population dynamics. The asymmetry
 620 of interaction strength leads to different dynamics in each patch that decreases the correlation of prey
 621 dynamics (Figure S2-13) and stabilises predator dynamics by decreasing their biomass CV (Figure S2-
 622 14A).

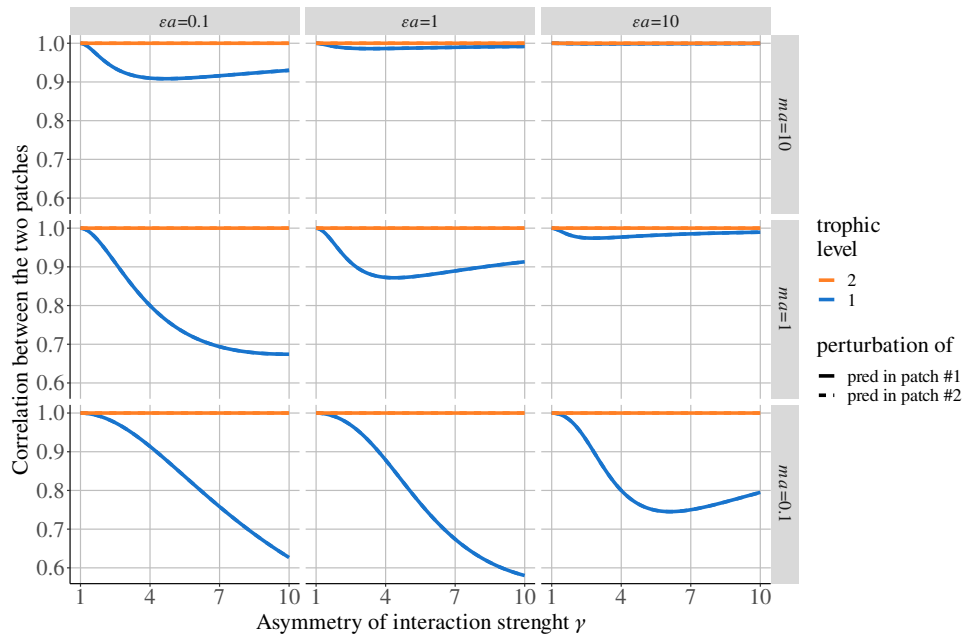


Figure S2-13: Correlation between populations depending on asymmetry of interaction strength γ , positive effect of prey on predator εa and negative effect of predator on prey ma . Predators disperse and are perturbed in patch #1 or patch #2 ($d_2 = 10^6$ and $\omega = \gamma$).

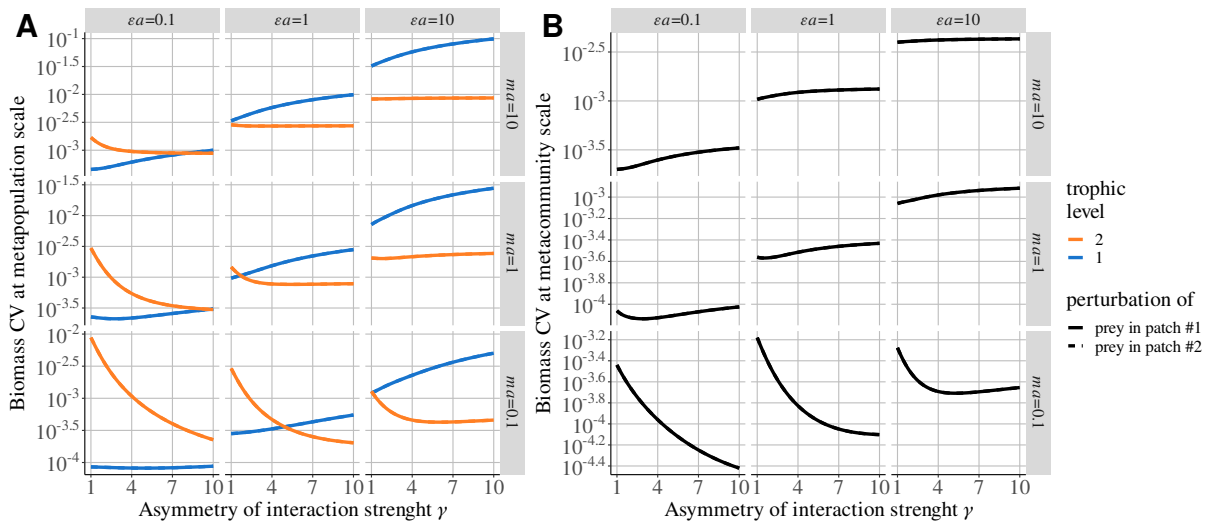


Figure S2-14: Biomass CV at different scales depending on asymmetry of interaction strength γ , positive effect of prey on predator εa and negative effect of predator on prey ma . Predators disperse and are perturbed in patch #1 or patch #2 ($d_2 = 10^6$ and $\omega = \gamma$). **A)** CV of the total biomass of each species. **B)** CV of the total biomass of the metacommunity.

623 S2-2-6 Effect of food chain length

624 Here, we consider three trophic levels to extend our results to metacommunities with longer food chain
 625 lengths. In this setup, only top predators (species 3) are able to disperse, and basal species (species 1)
 626 receive stochastic perturbations. γ also has the same value across trophic levels. We observe a similar
 627 response to the case with two trophic levels for the correlations of the dynamics of the biomass of species
 628 2 and 3 (Figure S2-15) as well as for biomass CV (Figure S2-16). However, the response of species 1

629 in completely different. Therefore, the mechanisms described in the main text are only acting for the
 630 dispersing species and the species directly interacting with it.

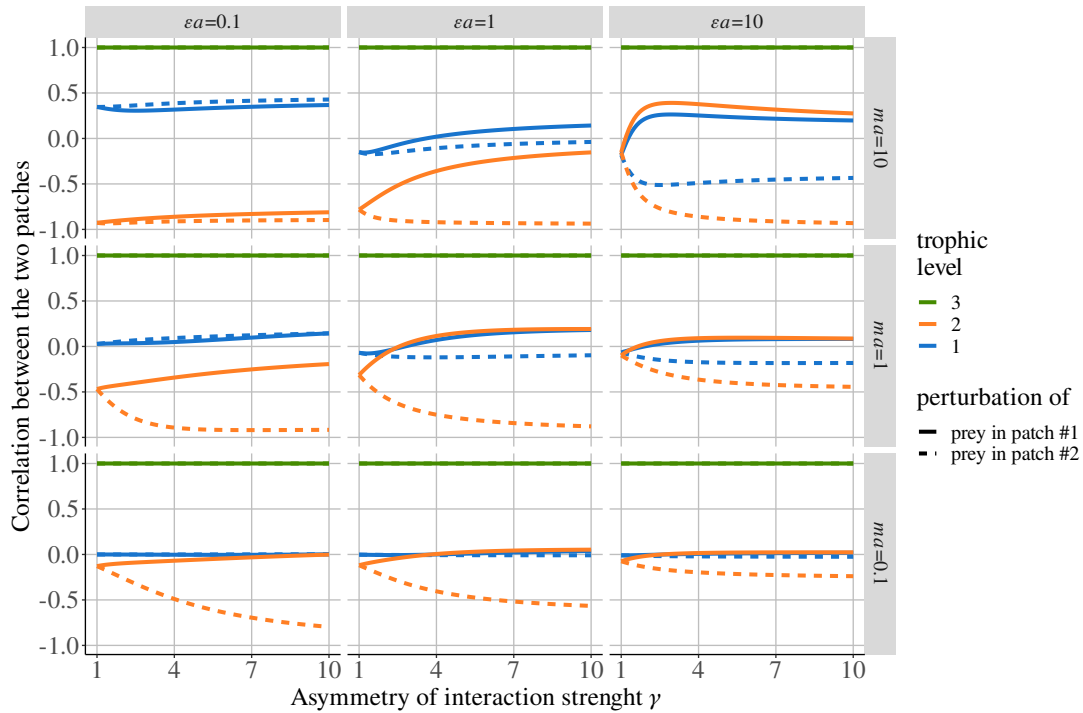


Figure S2-15: Correlation between populations in a three trophic level food chain depending on the asymmetry of interaction strength γ , positive effect of prey on predator ϵa and negative effect of predator on prey ma ($d_3 = 10^6$ and $\omega = 1$). Top predators disperse, and the basal species is perturbed in patch #1 or #2.

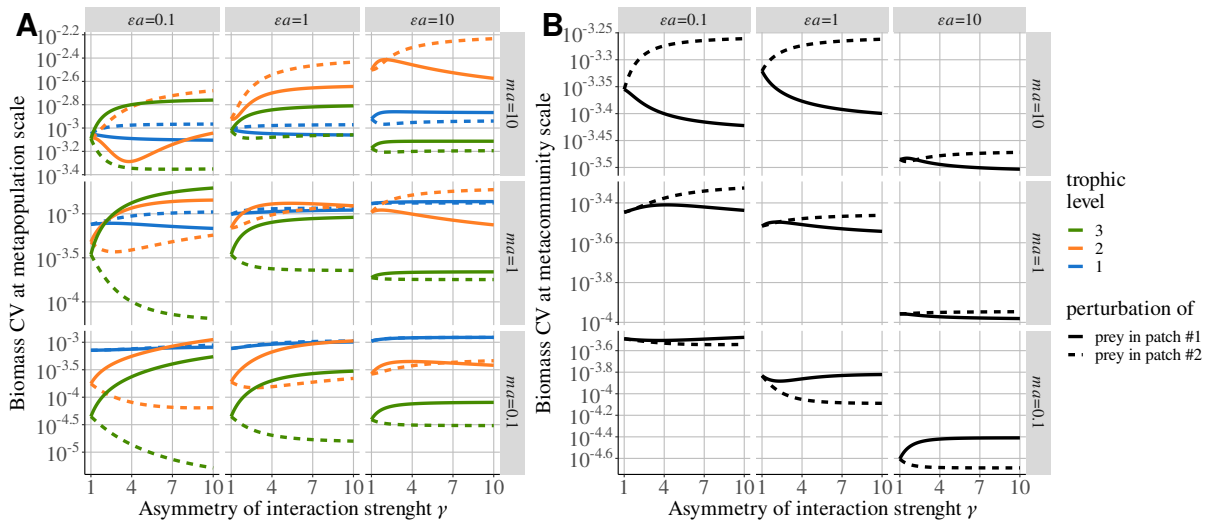


Figure S2-16: Biomass CV in a three trophic level food chain at different scales depending on asymmetry of interaction strength γ , positive effect of prey on predator ϵa and negative effect of predator on prey ma ($d_3 = 10^6$ and $\omega = 1$). **A**) Biomass CV of the population of each species in each patch. **B**) CV of the total biomass of each species.

631 S2-3 Dispersal of prey and perturbation of predators

632 In this section, we consider a setup mirroring the metacommunity model described in the main text.
 633 Here, only prey are able to disperse at a very high rate ($d_1 = 10^6$), and predators receive stochastic
 634 perturbations. We also set $\gamma = \omega$ to be consistent with the results in the main text. In the following,
 635 we find the same responses to the asymmetry of interaction strength γ , which demonstrates that the
 636 mechanisms described in the main text are not conditioned by the trophic position of the dispersing
 637 species.

638 S2-3-1 Conditions of coexistence

639 When only prey are able to disperse, all populations of each species have positive biomasses for all
 640 values of ω , γ , εa and ma (Figure S2-17).

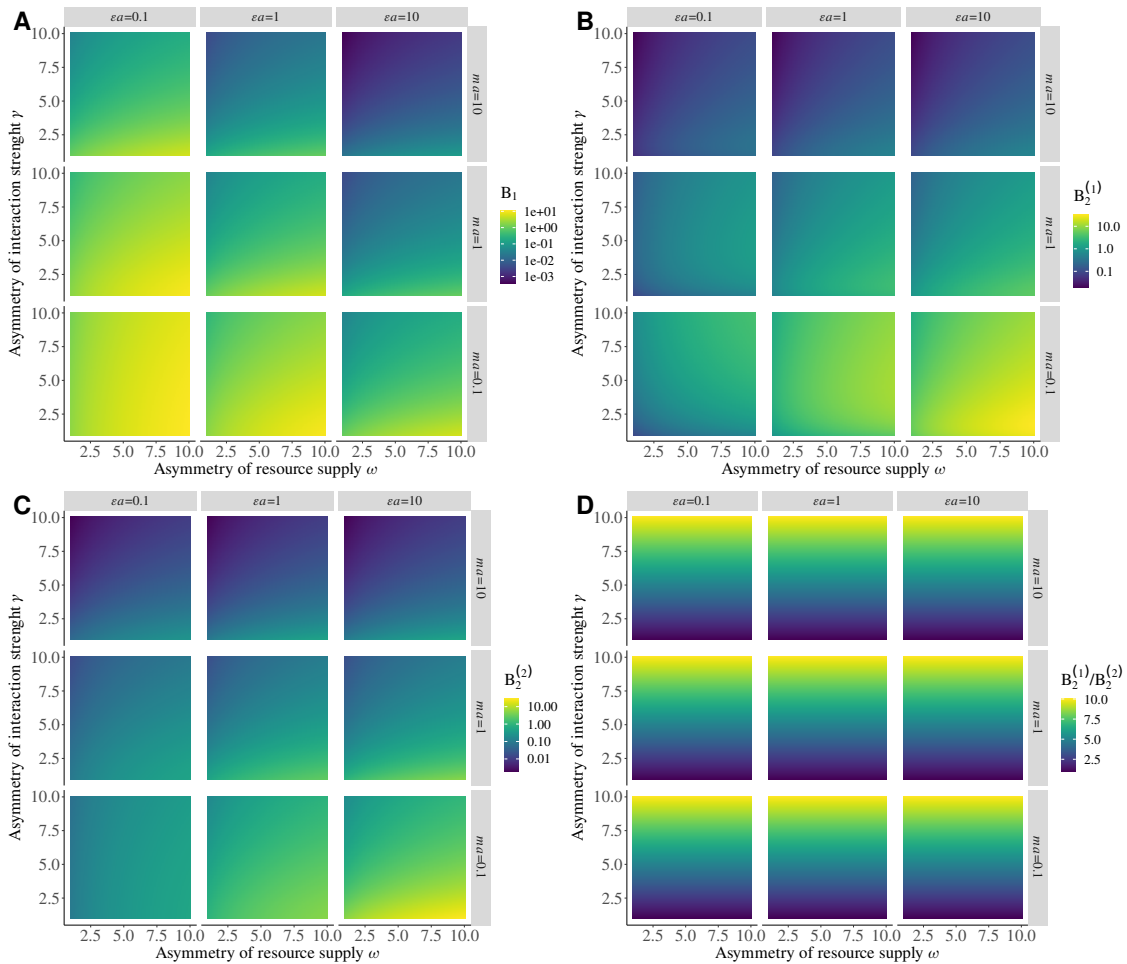


Figure S2-17: Distribution of parameters, asymmetry of resource supply ω and asymmetry of interaction strength γ , leading to the coexistence of predator and prey in each patch. Only prey are able to disperse at an infinite rate (well mixed prey populations). This distribution is assessed for different values of the positive effect of prey on predator εa and the negative effect of predator on prey ma . The product of εa and ma is the strength of top-down control λ ($\lambda = \varepsilon a^2 m$, see Barbier and Loreau (2019)). **A**) Biomass of prey in patches #1 and #2 ($B_1^{*(1)} = B_1^{*(2)}$) because prey populations are well mixed). **B**) Biomass of predator in patch #1 ($B_2^{*(1)}$) **C**) in patch #2 $B_2^{*(2)}$.

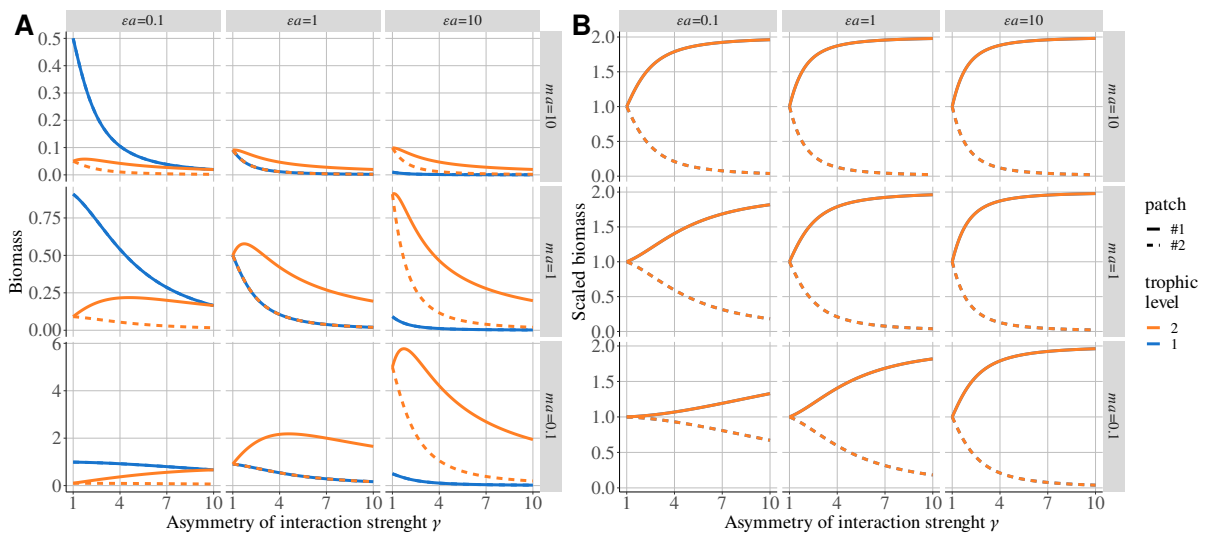


Figure S2-18: Biomass distribution of each species in each patch depending on asymmetry of interaction strength γ , positive effect of prey on predator εa and negative effect of predator on prey ma . **A)** Biomass distribution. **B)** Biomass scaled by the biomass in the metacommunity without dispersal ($d_1 = 0$). Prey and predator curves perfectly overlap

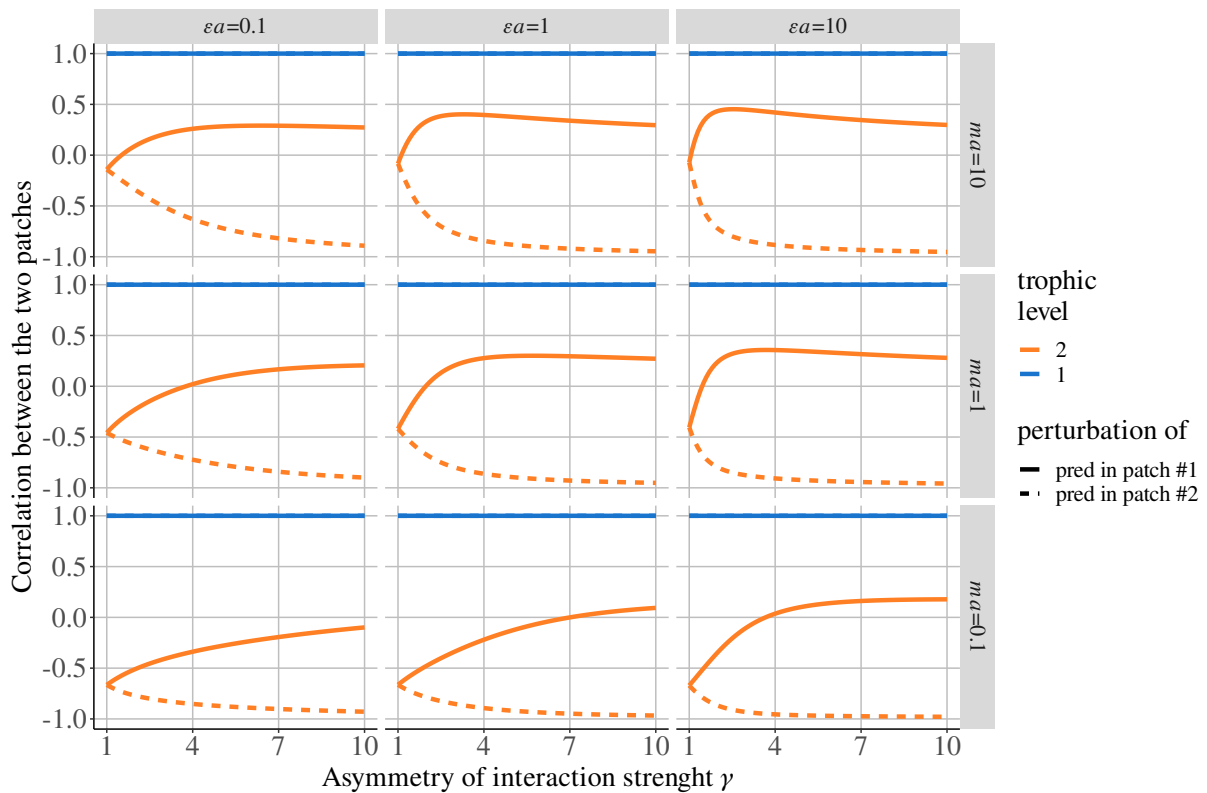


Figure S2-19: Correlation of population when prey disperse and predators are perturbed in patch #1 or in patch #2 depending on asymmetry of interaction strength γ , positive effect of prey on predator εa and negative effect of predator on prey ma .

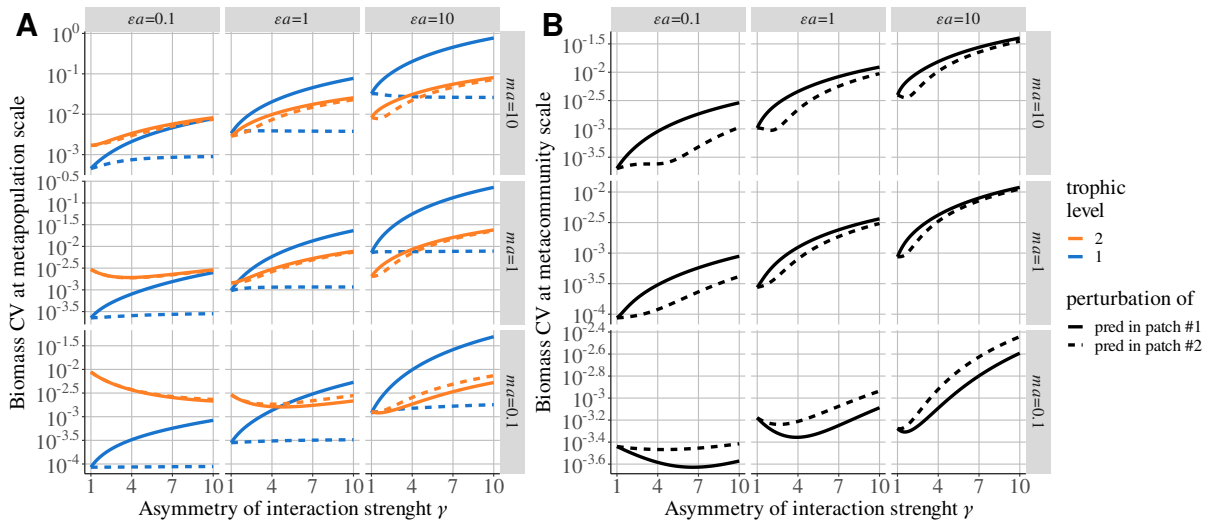


Figure S2-20: Biomass CV at different scales depending on asymmetry of interaction strength γ , positive effect of prey on predator ϵa and negative effect of predator on prey ma ($d_1 = 10^6$ and $\omega = \gamma$). **A**) Biomass CV of the population of each species in each patch. **B**) CV of the total biomass of each species.

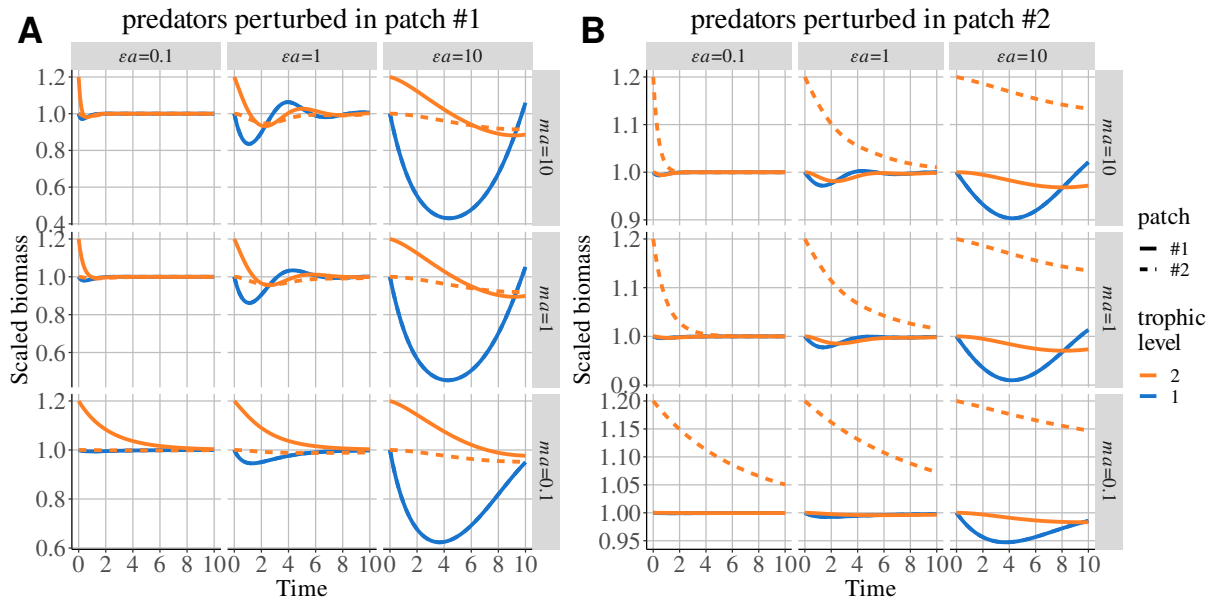


Figure S2-21: Time series after pulse perturbation of predators in patch #1 or in patch #2. Biomasses are scaled by their value at equilibrium, and dispersal is high ($\gamma = 3$ and $d = 10^6$).

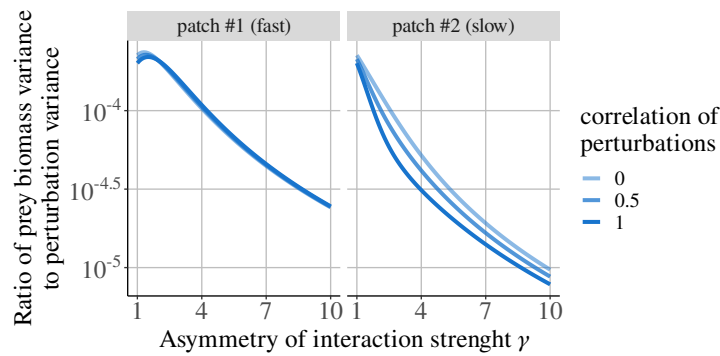


Figure S2-22: Ratio of the variance of prey biomass to the variance of environmental perturbations ($\text{Var}(B_i)/\sigma_i$) in each patch depending on asymmetry of interaction strength γ . Each prey population receives spatially correlated environmental perturbation (colour gradient scale) scaling with equilibrium biomass B_i^* .

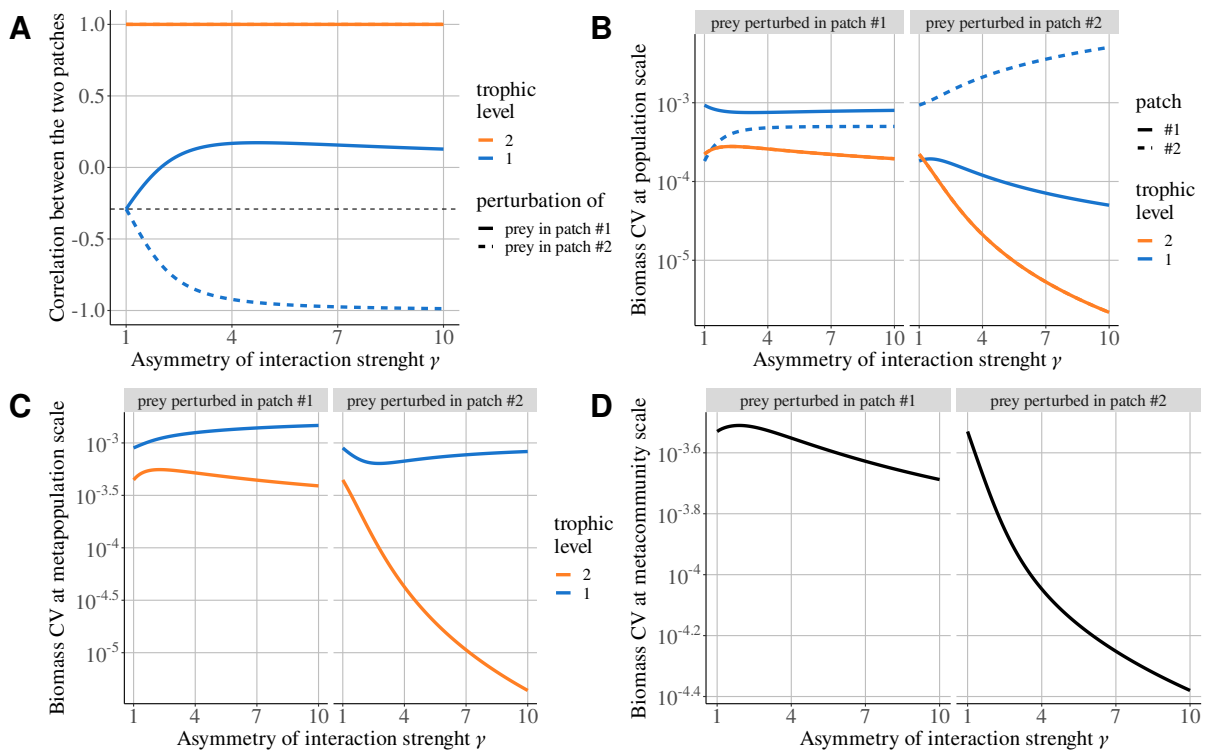


Figure S2-23: Stability at different scales depending on asymmetry of interaction strength γ when predators disperse and prey are perturbed in patch #1 or #2 with environmental perturbations ($\varepsilon a = 1$, $m a = 1$, $\omega = \gamma$). **A)** Spatial correlation between the populations of each species. **B)** Biomass CV at the population scale. **C)** Biomass CV at the metapopulation scale (CV of the total biomass of each species). **D)** Biomass CV at the metacommunity scale (CV of the total biomass of the metacommunity).

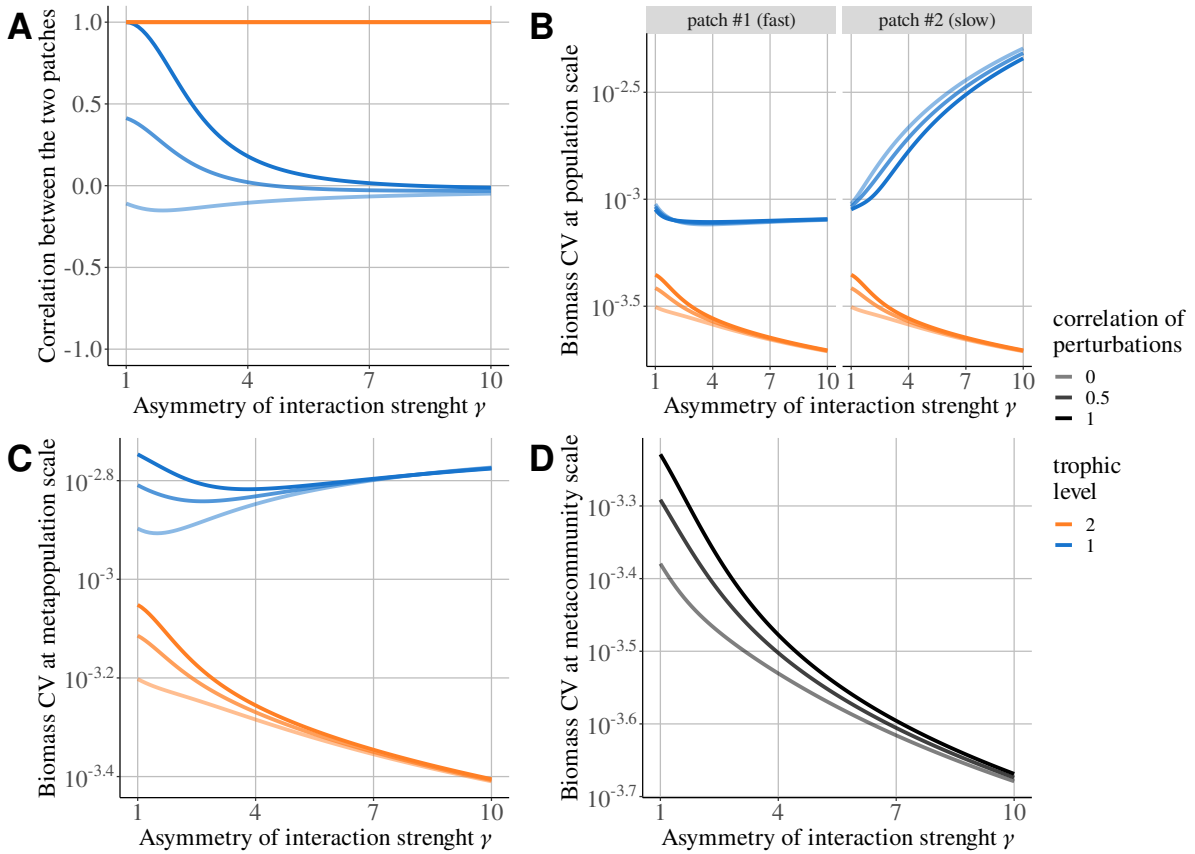


Figure S2-24: Stability at different scales depending on asymmetry of interaction strength γ when predators disperse and prey are perturbed by a spatially correlated environmental perturbations (colour gradient scale) ($\varepsilon a = 1$, $ma = 1$, $\omega = \gamma$). **A**) Spatial correlation between the populations of each species. **B**) Biomass CV at the population scale. **C**) Biomass CV at the metapopulation scale (CV of the total biomass of each species). **D**) Biomass CV at the metacommunity scale (CV of the total biomass of the metacommunity).

643 Here, we consider the same metacommunity as in the main text (see Figure 1 in the main text), but
 644 prey receive spatially correlated environmental perturbations. Environmental perturbations correspond
 645 to the synchronous response of all individuals of the same population to an environmental factor (*e.g.*,
 646 drought), and they scale with equilibrium biomass B_i^* (see the supporting information of Quévieux et al.
 647 (2021) for the demonstration). In our metacommunity, we also consider that environmental perturbations
 648 are spatially correlated since it is reasonable to assume that different populations of the same species will
 649 respond in a similar way to environmental perturbations.

650 The effect of a perturbation on a population can be assessed by the ratio of the variance of biomass
 651 to the variance of perturbations $\text{Var}(B_i)/\sigma_i$. As demonstrated by Arnoldi et al. (2019), environmental
 652 perturbations affect abundant populations the most, which is the prey population in the fast patch in
 653 our case (Figure S2-22). Therefore, we can approximate the effect of environmental perturbations by the
 654 effect of the perturbation of prey in the fast patch. Perturbing a single population with demographic or
 655 environmental perturbations leads to exactly the same qualitative results (Figure S2-23 and Figure 3 and

656 Figure 4 in the main text), and only the CV values change because of the different biomass scaling.

657 Increasing the correlation of perturbations increases the correlation of the dynamics of prey populations
 658 (Figure S2-24A) because of the Moran effect (Moran, 1953). The increase in synchrony explains the
 659 increase in the biomass CV observed at each scale for all species (Figure S2-24B-D), except for prey in
 660 the slow patch (Figure S2-24B). The Moran effect is particularly strong at low asymmetry ($\gamma < 4$), but
 661 once asymmetry is high enough, two mechanisms disrupt the Moran effect. First, when asymmetry is high,
 662 the dynamics in each patch become so different that correlated perturbations are not able to generate
 663 similar responses. Second, because of the discrepancy in the distribution of prey biomass among the two
 664 patches, environmental perturbations mostly affected prey in the fast patch (Figure S2-22). Therefore,
 665 with increasing asymmetry of interaction strength γ , the response of the metacommunity to correlated
 666 environmental perturbations converges towards the response of a metacommunity in which only prey in
 667 the fast patch are perturbed.

668 S2-5 Reminder of the symmetric case

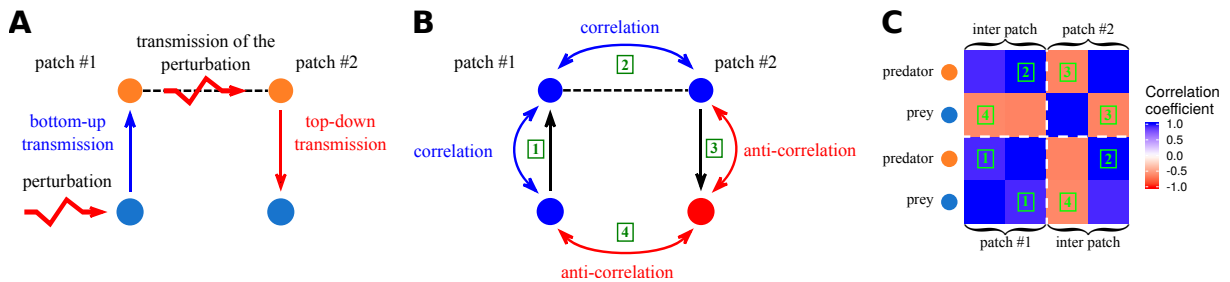


Figure S2-25: Summary of the main results from Quévieux et al. (2021), who considered a two patch predator-prey metacommunity with passive dispersal. In the setup presented in **A**), prey are perturbed in patch #1 and only predators are able to disperse. Thus, perturbations have a bottom-up transmission in patch #1 (*i.e.* transmission from lower to upper trophic levels). This leads to the temporal correlation of the biomass dynamics of predators and prey in patch #1 showed in **B**)(1) because if a perturbation increases the biomass of prey, it also increases the biomass of predators due to the vertical transfer of biomass. The passive dispersal of predators transmits the perturbations and spatially correlate their populations as shown in **B**)(2). Then, perturbations have a top-down transmission in patch #2 (*i.e.* transmission from upper to lower trophic levels). This leads to the temporal anticorrelation (negative coefficient of correlation) of the biomass dynamics of predators and prey in patch #2 showed in **B**)(3) because if a perturbation increases the biomass of predators, it decreases the biomass of prey due to the negative effect of predators on prey. Eventually, prey populations are spatially anticorrelated, as shown in **B**)(4). Hence, by knowing which species is perturbed, which species disperses and how perturbations propagate within a food chain, Quévieux et al. (2021) were able to explain the spatial synchrony of the various populations of a metacommunity, summarised by the correlation matrix in **C**).

669 References

- 670 Arnoldi, J.-F., Bideault, A., Loreau, M., & Haegeman, B. (2018). How ecosystems recover from pulse perturbations: A
671 theory of short- to long-term responses. *Journal of Theoretical Biology*, *436*, 79–92. <https://doi.org/10.1016/j.jtbi.2017.10.003>
- 672
- 673 Arnoldi, J.-F., Loreau, M., & Haegeman, B. (2019). The inherent multidimensionality of temporal variability: How common
674 and rare species shape stability patterns (J. Chase, Ed.). *Ecology Letters*, *22*(10), 1557–1567. <https://doi.org/10.1111/ele.13345>
- 675
- 676 Barbier, M., & Loreau, M. (2019). Pyramids and cascades: A synthesis of food chain functioning and stability. *Ecology*
677 *Letters*, *22*(2), 405–419. <https://doi.org/10.1111/ele.13196>
- 678 Haegeman, B., Arnoldi, J.-F., Wang, S., de Mazancourt, C., Montoya, J. M., & Loreau, M. (2016). Resilience, invariability,
679 and ecological stability across levels of organization. *bioRxiv*. <https://doi.org/10.1101/085852>
- 680 Moran, P. (1953). The statistical analysis of the Canadian Lynx cycle. *Australian Journal of Zoology*, *1*(3), 291. <https://doi.org/10.1071/ZO9530291>
- 681
- 682 Quévreur, P., Barbier, M., & Loreau, M. (2021). Synchrony and perturbation transmission in trophic metacommunities.
683 *The American Naturalist*, 714131. <https://doi.org/10.1086/714131>
- 684 Rooney, N., McCann, K. S., Gellner, G., & Moore, J. C. (2006). Structural asymmetry and the stability of diverse food
685 webs. *Nature*, *442*(7100), 265–269. <https://doi.org/10.1038/nature04887>